


ARTICLE

Expansion and differentiation of ex vivo cultured erythroblasts in scalable stirred bioreactors

Joan Sebastián Gallego-Murillo^{1,2}  | Giulia Iacono¹ | Luuk A. M. van der Wielen^{2,3} | Emile van den Akker¹ | Marieke von Lindern¹ | Sebastian Aljoscha Wahl²

¹Sanquin Research and Landsteiner Laboratory, Department of Hematopoiesis, Amsterdam UMC, Amsterdam, The Netherlands

²Department of Biotechnology, Faculty of Applied Sciences, Delft University of Technology, Delft, The Netherlands

³Bernal Institute, Faculty of Science and Engineering, University of Limerick, Limerick, Republic of Ireland

Correspondence

Marieke von Lindern, Sanquin Research and Landsteiner Laboratory, Department of Hematopoiesis, Amsterdam UMC, Plesmanlaan 125, Amsterdam 1066 CX, The Netherlands.
Email: m.vonlindern@sanquin.nl

Present address

Joan Sebastián Gallego-Murillo, Meatable, Alexander Fleminglaan 1, 2613AX, Delft, The Netherlands.

Sebastian Aljoscha Wahl, Lehrstuhl Für Bioverfahrenstechnik, Friedrich-Alexander Universität Erlangen-Nürnberg, Paul-Gordan-Str. 3, 91052, Erlangen, Germany.

Funding information

ZonMW TAS program, Grant/Award Number: 116003004; Landsteiner Foundation for Bloodtransfusion Research, Grant/Award Number: 1239; Sanquin Blood Supply, Grant/Award Numbers: PPOC17-28, PPOC19-14; European Union, Marie Skłodowska-Curie Innovative Training Networks, Grant/Award Number: 860436 (EVIDENCE)

Abstract

Transfusion of donor-derived red blood cells (RBCs) is the most common form of cell therapy. Production of transfusion-ready cultured RBCs (cRBCs) is a promising replacement for the current, fully donor-dependent therapy. A single transfusion unit, however, contains 2×10^{12} RBC, which requires large scale production. Here, we report on the scale-up of cRBC production from static cultures of erythroblasts to 3 L stirred tank bioreactors, and identify the effect of operating conditions on the efficiency of the process. Oxygen requirement of proliferating erythroblasts (0.55–2.01 pg/cell/h) required sparging of air to maintain the dissolved oxygen concentration at the tested setpoint (2.88 mg O₂/L). Erythroblasts could be cultured at dissolved oxygen concentrations as low as 0.7 O₂ mg/ml without negative impact on proliferation, viability or differentiation dynamics. Stirring speeds of up to 600 rpm supported erythroblast proliferation, while 1800 rpm led to a transient halt in growth and accelerated differentiation followed by a recovery after 5 days of culture. Erythroblasts differentiated in bioreactors, with final enucleation levels and hemoglobin content similar to parallel cultures under static conditions.

KEYWORDS

cell culture, cultured blood, erythropoiesis, red blood cell, scale-up, stirred tank bioreactor

Abbreviations: BM, bone marrow; CD235a, glycophorin A; CD49d, integrin alpha 4; CD71, transferrin receptor 1; cRBC, cultured red blood cell; Dex, dexamethasone; EDR, energy dissipation rate; Epo, erythropoietin; FC, fold change; HSC, hematopoietic stem cell; hSCF, human stem cell factor; NFATC2, nuclear factor of activated T-cells 2; OXPHOS, oxidative phosphorylation; PBMC, peripheral blood mononuclear cell; PBS, phosphate-buffered saline; PI, propidium iodide; RBC, red blood cell; rpm, revolutions per minute; SCF, stem cell factor; STAT5, signal transducer and activator of transcription 5A; STR, stirred tank reactor.

Marieke von Lindern and Sebastian Aljoscha Wahl share responsibility for the manuscript.

This is an open access article under the terms of the Creative Commons Attribution-NonCommercial-NoDerivs License, which permits use and distribution in any medium, provided the original work is properly cited, the use is non-commercial and no modifications or adaptations are made.

© 2022 The Authors. *Biotechnology and Bioengineering* published by Wiley Periodicals LLC.

1 | INTRODUCTION

Blood transfusion is the most common cell therapy to this date. Worldwide about 120 million blood donations, each containing 2×10^{12} red blood cells (RBC), are collected yearly. Nevertheless, availability of blood products for transfusion purposes is not uniformly distributed, with current shortages localized mostly in low-income countries (World Health Organization, 2021). Globalization and an increasing multiethnicity are societal factors that prompt for a larger, more diverse blood supply to ensure a safe transfusion practice (Klinkenberg et al., 2019; Vichinsky et al., 1990). Currently, over 360 blood group antigens are known, being part of more than 35 known blood group systems (Daniels, 2013). Finally, donor-dependent transfusion products harbor a risk for novel bloodborne pathogens that escape current screening programs.

Production of cultured red blood cells (cRBCs) represents a potentially unlimited source of RBCs for transfusion purposes, offering a better control on the quality and safety of the final product. Fully matched cRBCs could be used for patients that have developed alloimmunization or with rare blood groups (Pellegrin et al., 2021; Peyrard et al., 2011). Furthermore, cRBCs loaded with therapeutics or engineered to present antigens in their surface could be used as a highly efficient drug-delivery system (Koleva et al., 2020; Sun et al., 2017; Vichinsky et al., 1990; X. Zhang et al., 2021).

Our current *ex vivo* RBC culture protocol starts with peripheral blood mononuclear cells (PBMCs) and the commitment of CD34⁺ hematopoietic stem cells (HSCs) in this fraction to the erythroid lineage, which is characterized by high expression of the transferrin receptor (CD71). Subsequently, erythroblasts expressing glycophorin A (CD235a^{dim}), integrin- α 4 (CD49d^{dim-to-high}), and transferrin receptor 1 (CD71^{high}) are expanded in presence of erythropoietin (Epo) plus stem cell factor (SCF) and glucocorticoids (Heshusius et al., 2019; Migliaccio et al., 2002). The addition of SCF and glucocorticoids arrests differentiation and transiently enables renewal divisions of erythroblasts and expansion of a homogeneous erythroblast culture. Withdrawal of glucocorticoids and SCF allows for synchronous differentiation (Leberbauer et al., 2005; von Lindern et al., 1999).

Erythroid cells are commonly cultured in static dishes or flasks, in which spatial inhomogeneities in nutrient concentrations occur due to settling of cells to the bottom surface. Moreover, this cultivation system is susceptible to mass transfer limitations as transfer of oxygen to the culture is fully diffusion-dependent (Peniche Silva et al., 2020; Place et al., 2017; Sugiura et al., 2011). This type of culture systems would culminate in impractical numbers of dishes/flasks (currently about 9000–12,000 T175 flasks for a single transfusion unit) (Timmins & Nielsen, 2009, 2011).

The use of a static culture system in which oxygen transfer is facilitated by a gas-permeable membrane at the bottom of the vessel enabled a 50-fold increase in surface cell density (cells per cm²) compared to culture dishes (Heshusius et al., 2019). Nevertheless, scale up of this culture protocol is still by area, and limited control on culture conditions can be performed.

Cultivation systems mimicking the microstructure and micro-environment of the bone marrow (BM) niche were developed for cRBC production. Hollow fiber bioreactors enable tissue-like cell concentrations with continuous perfusion of fresh nutrients and dissolved oxygen (dO₂) (Allenby et al., 2019; Housler et al., 2012). Microcarriers and porous scaffolds are used, both under static (Severn et al., 2016, 2019) and agitated conditions (Lee et al., 2015). These biomimetic systems support high erythroblast cell densities. However, scale-up is hampered by gradients in nutrient concentrations along and across hollow fibers (Mohebbi-Kalhari et al., 2012; Piret et al., 1991) or inside microcarriers (Preissmann et al., 1997; Yu, 2012).

Active agitation of RBC cultures increases nutrient homogeneity and oxygen transfer. This includes roller bottles (Y. Zhang et al., 2017), rocking motion bioreactors (Boehm et al., 2010; Timmins et al., 2011), shake flasks (Aglialoro et al., 2021; Sivalingam et al., 2020), and spinner flasks (Griffiths et al., 2012; Kupzig et al., 2017; Sivalingam et al., 2020; Trakarnsanga et al., 2017). Stirred tank reactors (STRs) additionally allow for online monitoring and control of process parameters such as pH, dO₂, and nutrient concentrations. STRs are commonly used for suspension cultures of different mammalian cells such as CHO, HEK293, hybridoma, or Vero cell lines (Chu & Robinson, 2001; Rodrigues et al., 2010; Tapia et al., 2016), reaching volumes of up to ~20,000 L at an industrial scale (Farid, 2007). This type of reactors can be combined with cell retention systems, such as spin filters or external filtration systems, allowing for continuous culture processes with higher cell densities (Avgerinos et al., 1990; Karst et al., 2016).

For cRBCs, small scale STRs (15–500 ml) were used to explore the effects of several operating parameters (Han et al., 2021; Lee et al., 2018; Ratcliffe et al., 2012). Some studies reported a large increase in cell numbers. However, the conditions that were used varied widely with respect to medium composition, cell density, oxygenation, agitation (impeller type, speed), and nutrient feeding strategy between the different stages (Bayley et al., 2017; Han et al., 2021). In most of these cultures, expansion of the cell population was accompanied by differentiation. Erythroblasts undergo major changes during differentiation including reduction of mitochondria, and the change of an actin-based cytoskeleton to a spectrin/ankyrin-based cytoskeleton (K. Chen et al., 2009). Here, we applied defined bioreactor conditions that discriminate between expansion during transient renewal of erythroblasts, and subsequent differentiation to enucleated reticulocytes.

Shear stress is a relevant parameter in scale-up (Sieblist et al., 2016). The impact of shear stress on cultures seems to be cell-line dependent, affecting cell growth, viability, morphology, protein glycosylation, and differentiation fate (Godoy-Silva et al., 2009; Kretzmer & Schügerl, 1991; Wolfe & Ahsan, 2013; Wu, 1999). Shear stress in rocking culture plates or upon orbital shaking in Erlenmeyer flasks reduced erythroblast viability and accelerated erythroid differentiation (Aglialoro et al., 2021; Boehm et al., 2010). Enhanced differentiation is in agreement with increased enucleation and reduced cell proliferation reported for STRs (Bayley et al., 2017; Han et al., 2021). The effect of shear stress on erythroblasts may be

mediated, at least partially, by the mechanosensitive channel PIEZO1, which activates multiple calcium-dependent signaling transduction cascades including the Calcineurin-NFAT pathway, the modulation of signal transducer and activator of transcription 5A (STAT5) and ERK signaling, and inside-out integrin activation (Aglialoro et al., 2020; Aglialoro et al., 2021; Caulier et al., 2020).

Sparging can also represent a significant source of shear in bioreactor cultures, which is due to bubble formation, rise, and burst (Murhammer & Goochee, 1990; Villiger et al., 2015; Zhu et al., 2008). The negative effect of turbulence can be aggravated when higher stirring speeds and gas flow rates are needed upon scale-up to keep the cultures well-mixed with adequate oxygen supply (Xing et al., 2009). Nevertheless, it is still unclear if the observed negative effect of sparging on cell cultures is due to the mechanical forces generated during bubble coalescence and breakup, or by biochemical interactions between cells and air bubbles (Sobolewski et al., 2011; Walls et al., 2017; Walsh et al., 2017).

Oxygen availability is a critical parameter in mammalian cell cultures. Cell cultures are often performed under dO_2 concentrations that are higher than those *in vivo*, potentially leading to an increase in oxidative stress, decrease in growth rate, acceleration of cell differentiation, and increase in apoptosis (Mas-Bargues et al., 2019). *In vivo*, erythroblasts are exposed to the hypoxic conditions of the extravascular BM niche, with a mean oxygen partial pressure of 13.3 mmHg (range: 4.8–21.1 mmHg; (Spencer et al., 2014)), equivalent to a dO_2 concentration of 0.6 mg O_2/L (range: 0.2–0.9 mg O_2/L), or a 8% (range: 3%–13%) of saturation in equilibrium with air (1 atm, 37°C).

Low oxygen pressure in static culture conditions accelerated erythroblast differentiation, increased hemoglobin levels and the enucleation rates, and increased the expression of the hypoxia-inducible factor 1 α (Bapat et al., 2021; Goto et al., 2019). Vlaski et al. (2009) also reported accelerated erythroid differentiation, but an increased cell yield in the first culture stage, using gas oxygen concentrations as low as 1.5%. However, it is difficult to predict the local dO_2 concentrations to which cells are exposed in the culture dishes used for these experiments, as static culture systems often display dO_2 gradients (Place et al., 2017). In contrast, a more homogeneous dO_2 concentration can be monitored and controlled in STR cultivations using in-line oxygen measurements. The effect of dO_2 on enucleation and cell yields in STR erythroid cultures depends on other process parameters such as pH, temperature, and shear (Han et al., 2021).

Oxygen requirements of erythroid cultures are dynamic during the maturation process, with cells switching between oxidative phosphorylation (OXPHOS) and glycolysis (Richard et al., 2019). Although oxygen requirements of mature RBCs are well known, there is limited data for erythroid precursors at specific developmental stages. Oxygen consumption rates for erythroblast have been estimated in Seahorse assays, ranging between 0.26 and 1.66 pg/cell/h (Caielli et al., 2021; Gonzalez-Menendez et al., 2021; Jensen et al., 2019). Erythroblast oxygen requirements in STR cultures range between 0.06 and 0.21 pg/cell/h (cell-specific oxygen consumption

rate; q_{O_2}), and go as low as 0.01–0.05 pg/cell/h in the later stages of differentiation (Bayley et al., 2017).

In the present study, we report the implementation of our cRBC culture protocol in STRs. As oxygen availability was identified as a critical parameter controlling the yields of cRBCs, we estimated the oxygen requirements of erythroblasts during their transient renewal phase, and evaluated the effect of dO_2 and stirring speed on cell yields during erythroblast expansion and differentiation in this culture system. Based on appropriate culture conditions identified in 0.5 L STRs, we were able to scale up to 3 L STRs, maintaining the same proliferation and differentiation efficiency. To our knowledge, this is the first report of erythroid cultivation in STR bioreactors at >1 L scale, and taking the differentiation stage into account.

2 | MATERIALS AND METHODS

2.1 | Cell culture

Human adult PBMCs were purified by density centrifugation using Ficoll-Paque (density = 1.077 g/mL; 600 g, 30 min; GE Healthcare). Informed written consent was given by donors for the use of waste material for research purposes, and was checked by Sanquin's NVT Committee (approval file number NVT0258; 2012) in accordance with the Declaration of Helsinki and the Sanquin Ethical Advisory Board. RBCs were cultured from PBMCs as previously described (Heshusius et al., 2019), with minor modifications: nucleosides and trace elements were omitted; cholesterol, oleic acid, and L- α -phosphatidylcholine were replaced by a defined lipid mix (1:1000; Sigma-Aldrich cat#L0288). Expansion cultures were supplemented with Epo (1 U/ml; EPREX[®]; Janssen-Cilag), human stem cell factor (hSCF; 50 ng/ml, produced in HEK293T cells), dexamethasone (Dex; 1 μ mol/L; Sigma-Aldrich), and interleukin-3 (1 ng/ml, first day only; Stemcell Technologies). Cell density was maintained between 0.7 and 2×10^6 cells/ml by daily feeding with fresh expansion medium (either increasing the liquid volume with the addition of fresh medium, or keeping the liquid volume constant by harvesting a fraction of the culture and adding a respective volume of fresh medium).

To induce differentiation, cells were washed and reseeded at 1×10^6 cells/ml in Cellquin medium supplemented with Epo (5 U/ml), 5% Omniplasma (Octapharma GmbH), human plasma-derived holo-transferrin (1 mg/ml; Sanquin), and heparin (5 U/ml; LEO Pharma A/S). Cells were kept in culture for 11 days, without medium refreshment, until fully differentiated, in either stirred bioreactors or in culture dishes.

2.2 | Bioreactor and reference culture conditions

All cultivations were performed on either autoclavable (MiniBio 500 ml, or 2 L single wall; glass) or single-use (AppliFlex 0.5 L, or AppliFlex 3.0 L; plastic) stirred bioreactors (Applikon Biotechnology B.V.). For expansion cultures, PBMC-derived erythroblast cultures of

at least 150 ml, with a density of $0.7\text{--}0.9 \times 10^6$ cells/ml were seeded in bioreactors. With the usual seeding methods of PBMC, the required amount was reached between Days 8 and 10. In presence of SCF and Dex, the differentiation stage of the cells remained similar independent of the cultivation duration. The cell concentration was measured every 24 h, and partial media refreshment was performed if the measured cell density was $>1.2 \times 10^6$ cells/ml, diluting the cell culture to 0.7×10^6 cells/ml. For differentiation cultures, cells were seeded at 1×10^6 cells/ml and cultured without medium additions.

Process control was established using PIMS Lucillus (Securecell AG). Cultures were agitated using a marine impeller (down-pumping) at defined stirring speeds. pH was measured using an AppliSens pH+ probe (AppliSens) and kept at 7.5 by sparging CO_2 (acid), as culture medium is carbonate-buffered (34.3 mM dissolved NaHCO_3). pH probe drift was corrected by recalibration every 2 days using an off-line pH measurement. dO_2 concentration was monitored using a polarographic probe (AppliSens), and was controlled by sparging pure air using a porous sparger (average pore size = 15 μm). dO_2 values are reported as the percentage relative to the oxygen saturation concentration in water at equilibrium with air (1 atm, 37°C; 100% = 7.20 mg O_2 /L).

Unless indicated otherwise, 0.5 L STR cultures were performed keeping the working volume constant at 300 ml, with a stirring speed of 200 revolutions per minute (rpm) using a marine impeller of diameter 2.8 cm. A constant headspace flow of N_2 (100 ml/min) was used during the whole cultivation to strip excess CO_2 or O_2 from the culture.

Static dish cultures (at 37°C, air + 5% CO_2 atmosphere) were used in parallel as reference for all tested conditions, with the same inoculum, growth media, and seeding/feeding regime performed as in the bioreactors. The dishes surface was 60.1 cm^2 , containing 12 ml of medium (liquid height = 2 mm).

2.3 | Cell characterization

2.3.1 | Cell count and viability

Cell density was measured in triplicate using an electrical current exclusion method at a size range of 7.5–15 and 5–15 μm in expansion and differentiation cultures, respectively (CASY Model TCC; OLS OMNI Life Science; or Z2 Coulter Counter; Beckman Coulter). Population fold change (FC) was calculated in reference to cell numbers at the start of the growth experiments: $\text{FC} = N(t_{i+1})/N(t_0)$. Viability was determined using a hemocytometer and a dye exclusion method (Trypan Blue; Sigma-Aldrich).

2.3.2 | Differentiation and viability measurements using flow cytometry

About 200,000 cells were stained in 4-(2-hydroxyethyl)-1-piperazineethanesulfonic acid buffer + 0.5% bovine serum albumin (30 min, 4°C), measured using an BD FACSCanto™ II or Accuri C6

flow cytometer (BD Biosciences), gated against specific isotypes, and analyzed using FlowJo™ (version 10.3). Antibodies or reagents used were: (i) CD235a-PE (1:2500 dilution; OriGene cat#DM066R), CD49d-BV421 (1:100 dilution; BD-Biosciences cat#565277), DRAQ7 (live/dead stain; 1:200 dilution; Thermo Fischer Scientific cat#D15106); (ii) CD235a-PE (1:2500 dilution; OriGene cat#DM066R), CD71-APC (1:200 dilution; Miltenyi cat#130-099-219); (iv) propidium iodide (PI) (live/dead stain; 1:2000 dilution; Invitrogen cat#P3566); (v) AnnexinV-FITC (1:1000 dilution; BioLegend cat#640906), DRAQ7 (live/dead stain; 1:200 dilution; Thermo Fischer Scientific cat#D15106); (vi) DRAQ5 (nuclear stain; 1:2500 dilution; abcam cat# ab108410). Stainings with panels (iv), (v), and (vi) were performed 10 min before analysis without intermediate washing steps.

2.3.3 | Cell morphology and hemoglobin content

Cell pellets (2.5×10^6 cells, after centrifugation for 5 min at 600 g) were washed with phosphate-buffered saline (PBS), resuspended in PBS + 5% human serum albumin, and smeared onto microscope slides. Slides were left to air overnight, stained with Hemacolor® Rapid Staining (Sigma-Aldrich), mounted with Entellan® (Merck), and examined by bright field microscopy (Leica DM5500B; Leica Microsystems). Hemoglobin content was determined using o-phenylenediamine as previously described (Bakker et al., 2004).

2.3.4 | Lactate and ammonium measurements

Cell culture samples were taken daily before and after medium refreshment. After centrifugation (600 g, 5 min), the supernatant was snap frozen in liquid nitrogen and stored at -80°C until further analysis. Upon thawing, lactate concentrations were measured using a RAPIDlab 1265 blood analyzer (enzymatic amperometric biosensor; Siemens Healthineers). Ammonium concentration was determined via an enzymatic spectrophotometric assay (Sigma-Aldrich cat#AA0100). Average daily growth rate (μ_{max}), doubling time ($t_{1/2}$), and the cell-specific metabolite consumption or production rates (q_{lac} , q_{NH_4}) were calculated as described in Supporting Information: Methods.

2.3.5 | Oxygen consumption rate determination

For the determination of the oxygen consumption rate of proliferating erythroblast, bioreactor cultures were run at 200 rpm, with no sparging (no active pH or dO_2 control), and with a fixed overhead flow of 100 ml/min air + 5% CO_2 as only source of oxygen. pH was continuously monitored, and passively controlled by the equilibrium between CO_2 in the overhead and the sodium bicarbonate present in the culture medium (pH variation between 7.2 and 7.7 during the cultivation). The cell-specific consumption rate of oxygen (q_{O_2}) for each day of culture was determined by the dynamic method, fitting

the measured dO_2 data as described in Supporting Information: Methods and using the experimentally determined mass transfer coefficient of the system ($k_{La} = 0.82$ 1/h) at the culture conditions.

2.4 | Statistical analysis

Statistical analyses were performed using unpaired two-tailed two-sample equal-variance Student's *t*-test. All data in figures represent the mean \pm the standard deviation of the measurements. The number of replicates is $N = 3$ for all experiments, unless indicated.

3 | RESULTS

3.1 | Oxygen consumption by proliferating erythroblasts

To determine the feasibility of erythroblast proliferation in stirred tank bioreactors (STRs), Day 9 PBMC-derived erythroblast cultures were seeded in a 2 L STR (working volume = 1 L). Cells were cultured with a stirring speed of 50 rpm (marine impeller; tip speed = 118 mm/s), with air diffusion from the headspace as the sole source of oxygen for the cell culture, similarly to aeration in static culture dishes and orbital shaking (Aggialoro et al., 2021; Heshusius et al., 2019). We observed complete depletion of oxygen after 6–12 h in the bioreactor culture, followed by a decrease in cell growth and viability compared to a parallel culture in dishes after 24 h (Figure 1a–c; representative experiment). Continuous sparging of air + 5% CO_2 caused excessive foam production, with cell debris accumulating in foam (data not shown). Proliferation and viability were restored to levels similar or better compared to those of static cultures when headspace aeration was complemented with sparging triggered when the measured dO_2 concentration was lower than 2.88 mg O_2 /L (equivalent to 40% of saturation with air; a setpoint typically used in STR mammalian cell cultures; Jan et al., 1997; Ozturk & Palsson, 1991; Restelli et al., 2006; Figure 1b,c). No foaming was observed under these conditions.

The results prompted to measure the oxygen consumption, for which smaller culture volumes were used (in standardized 0.5 L bioreactors) with headspace aeration (100 ml/min of air + 5% CO_2) and an increased stirring speed (200 rpm; marine impeller; tip speed = 293 mm/s). Day 9 expansion cultures, established from PBMCs, were measured throughout 6 subsequent days of proliferation. Cell numbers were assessed daily, and cultures were diluted with fresh medium, transiently increasing the oxygen concentration (Figure 1d,e). A wide variation of dO_2 was observed, going from as high as 100% of saturation after medium refreshment, to as low as 10% when high cell concentrations were reached. Oxygen was not limiting in these cultures, due to the higher mass transfer coefficient ($k_{La} = 0.82$ 1/h), and the lower total oxygen demand because of the lower culture volume. The cell-specific oxygen consumption rate (q_{O_2}) was calculated for five independent cultures at distinct days (Supporting Information: Methods) and decreased from 2.01 ± 0.53 at

the start of the experiment (Day 9 of culture) to 0.55 ± 0.24 pg/cell/h 6 days later (Figure 1f; Supporting Information: Figure S1). The decrease in oxygen consumption mirrored a decrease in cell proliferation (Figure 1d). It was shown earlier that cultures undergo limited spontaneous differentiation (as measured in the increase of $CD235a^+/CD71^{low}$ cells), reducing the expansion rate of the erythroblast population (Heshusius et al., 2019). Moreover, differentiating erythroblasts require less oxygen (Bayley et al., 2017). Such enhanced spontaneous differentiation of erythroblasts could explain both the reduced proliferation and decreased oxygen consumption.

Although headspace aeration can ensure oxygen availability in 0.5 L bioreactor cultures, a faster aeration system will be required to ensure sufficient O_2 supply in cultures with increased volume or higher cell density. Additionally, due to the limited transfer rate, the dO_2 level cannot be controlled well using headspace aeration only (i.e., long response times), which makes the evaluation of the effect of specific dO_2 concentrations on erythroblast cultures challenging.

3.2 | Controlled aeration supports erythroblast expansion in stirred tank bioreactors

To improve the dO_2 control in 0.5 L bioreactors, we used intermittent sparging of air, combined with a continuous headspace flow of nitrogen (100 ml N_2 /min) to strip excess O_2 from the culture and drive dO_2 to the desired setpoint (40% dO_2) (Supporting Information: Figure S2A). Intermittent sparging of CO_2 controlled the pH (=7.5; Supporting Information: Figure S2B).

Day 9 PBMC-derived erythroblast cultures were seeded in the bioreactors at an initial cell concentration of 0.7×10^6 cells/ml (Figure 2a). Erythroblasts seeded in culture dishes were cultured in parallel using similar medium refreshment conditions as reference.

The growth profile was comparable between bioreactor and static cultures, showing a 750-fold increase in cell number after 10 days of culture (resp. Days 9–18 counting from PBMC isolation and seeding; Figure 2b). No significant difference was found between the viability of bioreactor and dish cultures (Day 10 PI^- events: $92.9 \pm 1.1\%$ in bioreactors, $94.5 \pm 0.4\%$ in culture dishes; Figure 2c). Flow cytometry indicated that most cells were committed to the erythroid lineage at the start of the bioreactor culture ($<10\%$ $CD235a^-/CD71^-$ cells; $>70\%$ $CD235a^+$; Figure 2d; gating strategy available in Supporting Information: Figure S3). Although sustained proliferation of $CD235a^+/CD49d^+/CD71^{high}$ erythroblasts can be maintained in presence of EPO, hSCF, and Dex, some spontaneous differentiation can take place, initially leading to an increase in $CD235a^+$ cells, and a subsequent gradual decrease of $CD49d$ and $CD71$ expression. Both in bioreactors and dishes the percentage of $CD235a^+/CD71^{low}$ and $CD235a^+/CD49d^-$ cells was maintained lower than 10% during the whole cultivation (Figure 2d,e). During the last 5 days of the experiment (Days 14–19 after seeding PBMCs), the mean cell diameter gradually decreased (Figure 2f). Staining with AnnexinV and DRAQ7 indicated only a low percentage of apoptotic or dead cells (Supporting Information: Figure S3D), whereas cytopins indicated a large portion of cells with condensed nuclei (Figure 2g),

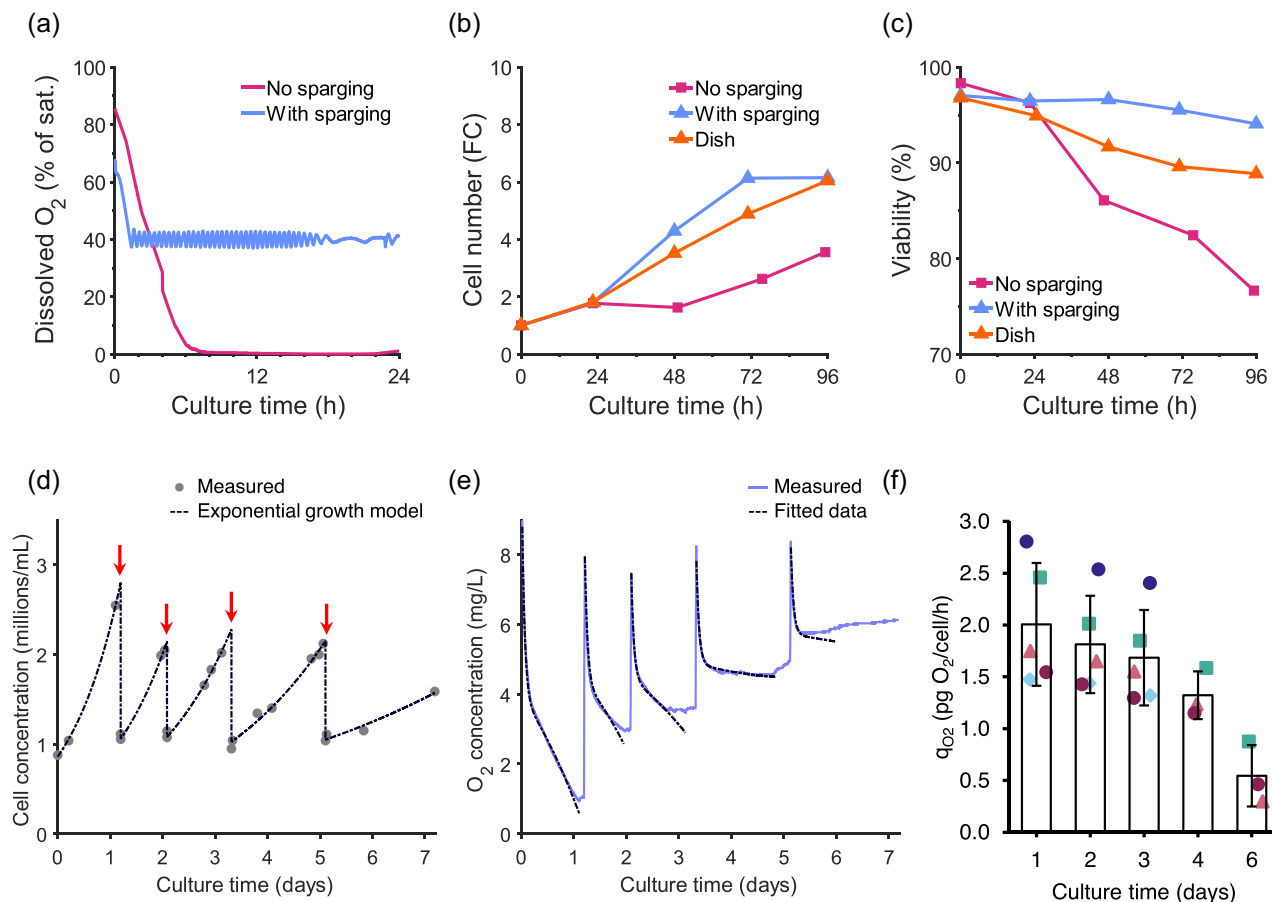


FIGURE 1 Oxygen can be limiting for erythroblast proliferation in stirred tank bioreactors when headspace aeration is used as sole O_2 source. (a)–(c) Erythroblasts were expanded from PBMCs for 9 days, and subsequently seeded in culture dishes (orange line) or in a 1.5 L STR (working volume: 1 L; stirring speed: 50 rpm; marine down-pumping impeller, diameter: 4.5 cm; 37°C), in which oxygen was provided by gas flow (air + 5% CO_2) in the headspace (0.3 L/min; purple line, no sparging), or by intermittent sparging triggered at <40% dissolved oxygen (dO_2 : % of the oxygen saturation concentration at the culture conditions; blue line), while pH (~7.20) was maintained by bicarbonate-buffered medium in equilibrium with the headspace gas. (a) dO_2 concentration in the culture was measured continuously. (b) Erythroblast cell concentration was monitored daily. Cells were diluted with fresh medium if the measured cell concentration was $>1.2 \times 10^6$ cells/ml. Fold change (FC) in cell number was calculated relative to the number of erythroblasts at the start of culture. (c) Culture viability was determined using a trypan blue dye exclusion method. (a)–(e) show data for a representative reactor run. (d)–(f) To determine the oxygen requirements of proliferating erythroblasts, Day 9 cells were inoculated in 0.5 L STRs (working volume: 300 ml; stirring speed: 200 rpm; marine down-pumping impeller, diameter: 2.8 cm), with a headspace flow of 100 ml/min (air + 5% CO_2) as only source of oxygen for the culture. (d) A constant growth rate was fitted for each time interval between consecutive medium refreshment events. (e) The drop of dO_2 after each medium refreshment was used to estimate the cell-specific oxygen consumption rate (q_{O_2}) for each time interval, using the experimentally determined mass transfer coefficient ($k_L a$) of 0.82 1/h (see Supporting Information: Methods). (f) The average cell-specific oxygen consumption rate, q_{O_2} , during erythroblast expansion was calculated as the mean of at five independent bioreactor runs (time intervals for which the q_{O_2} was calculated for each run available in Supporting Information: Figure S1). PBMC, peripheral blood mononuclear cell; STR, stirred tank reactor.

indicative of spontaneous differentiation. Thus, spontaneous differentiation, rather than decreased viability, reduced the proliferative capacity of Days 17–19 cultures. Importantly, this was similar between static cultures and cells cultured in bioreactors.

3.3 | Effect of dO_2 concentration on erythroblast expansion cultures

Standard mammalian cell culture conditions are mostly hyperoxic compared to their native in vivo niche, potentially leading to oxidative

stress and impaired growth (Mas-Bargues et al., 2019). The 40% dO_2 used in our initial experiments, equivalent to 2.88 mg O_2 /ml, is fivefold higher than the oxygen concentration in the BM compartment in which erythroblast proliferation and differentiation takes place (0.6 mg O_2 /ml; Spencer et al., 2014). Therefore, we tested whether BM mimicking oxygen concentrations also supported erythroblast expansion. Bioreactor cultures at 10% dO_2 (0.72 mg O_2 /L) showed comparable cell yields to dish conditions (Figure 3a), while requiring lower volumes of sparged air compared to 40% dO_2 (Supporting Information: Figure S4A). A continuous decrease of growth rate, from 0.78 ± 0.19 to 0.45 ± 0.05 1/day after

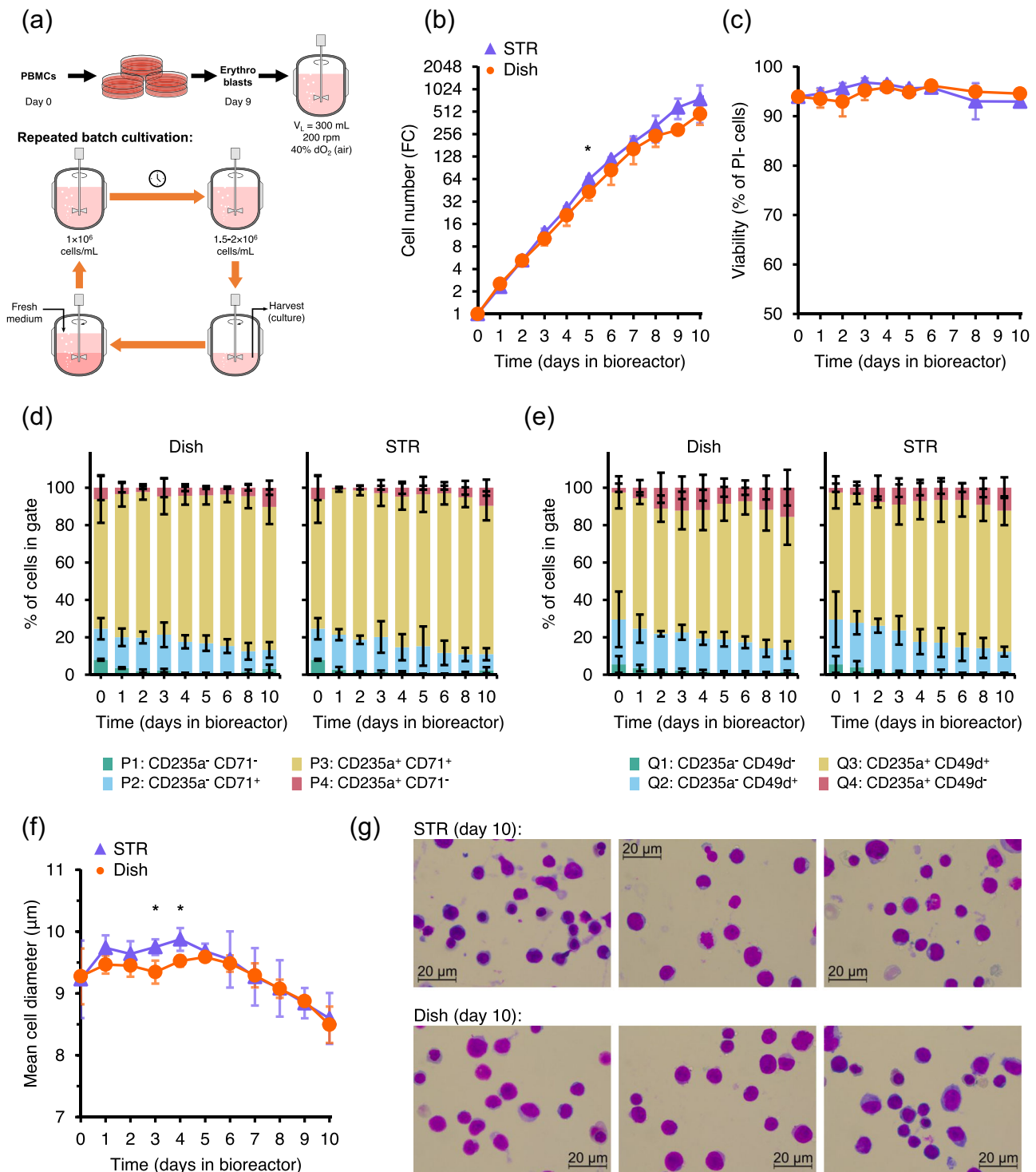


FIGURE 2 Efficient expansion of erythroblasts can be achieved in stirred tank bioreactors. Erythroblasts were expanded from PBMCs for 9 days, and subsequently seeded in culture dishes (orange lines) or STRs (blue lines) at a starting cell concentration of 0.7×10^6 cells/mL. STRs were run with a constant N_2 headspace flow to fully control dO_2 and pH. (a) Cells were cultured using a sequential batch feeding strategy: medium was refreshed when the cell concentration (measured daily) was $>1.2 \times 10^6$ cells/mL. (b) Cell concentration during 10 days of expansion (fold change [FC] compared to start of the culture). (c)–(e) Cells were stained with propidium iodide (PI); the percentage of PI⁻ cells indicate the % of viable cells (c), and with CD235a plus CD71 (d), or CD235a plus CD49d (e) (gating strategy available in Supporting Information: Figure S3). (f) Mean cell diameter (of cells $>5 \mu$ m) was measured daily. (g) Cytospin cell morphology by May-Grünwald-Giemsa (Pappenheim) staining of cultures after 10 days of expansion. All data are displayed as mean \pm SD (error bars; $n = 3$ reactor runs/donors). Significance is shown for the comparison with dish cultures (unpaired two-tailed two-sample equal-variance Student's t -test; * $p < 0.05$, not displayed if difference is not significant). dO_2 , dissolved oxygen; PBMC, peripheral blood mononuclear cell; STR, stirred tank reactor.

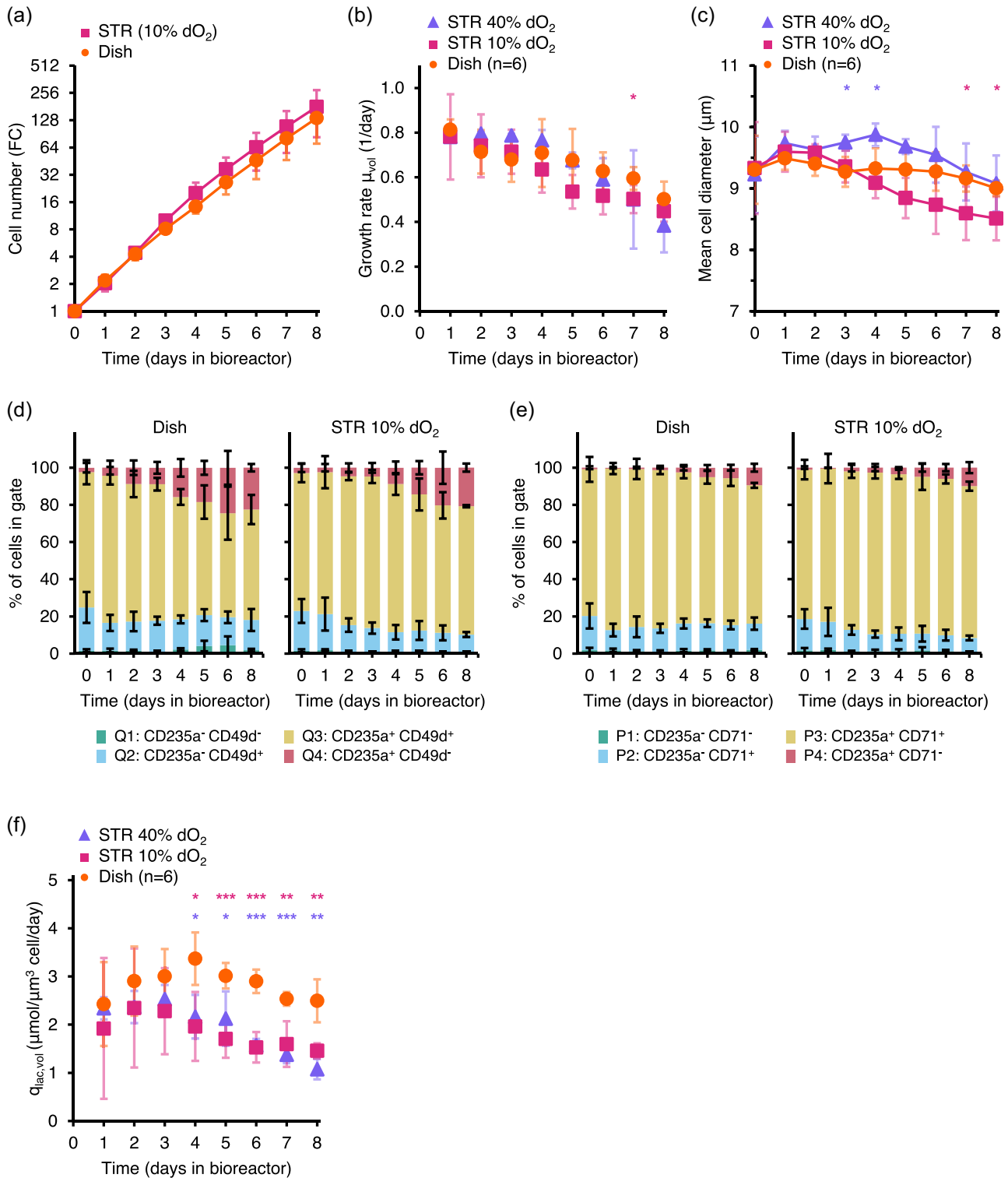


FIGURE 3 (See caption on next page)

8 days of culture, was observed in bioreactor cultures at 10% dO₂. By contrast, in hyperoxic bioreactor cultures (dO₂ = 40%) the growth rate was stable at ~0.78 1/day for the first 5 days of culture, followed by a decrease to 0.38 ± 0.12 1/day at Day 8 of cultivation (Figure 3b; growth rates calculated using cell counts available in Supporting Information: Figure S4C).

Cell size also decreased faster during the culture period at 10% dO₂ (Figure 3c). This may indicate partial differentiation within the population of CD235a⁺/CD71⁺/CD49d⁺ population, or a reduced protein synthesis at this lower O₂ concentration (Brugarolas et al., 2004). Although the percentage of CD235a⁺/CD49d⁻/CD71^{low} cells increased during culture, this was similar between bioreactors at 10% dO₂ and standard static cultures (Figure 3d,e). Lactate, typically produced by aerobic glycolysis and glutaminolysis, may negatively influence erythroblast growth and viability. Extracellular lactate concentrations were typically <6 mM during culture in bioreactors or culture dishes (Supporting Information: Figure S2E). Nevertheless, a consistently lower cell-specific lactate production rate (q_{lac,vol}) was observed in bioreactor conditions both at 10% and 40% dO₂, compared to culture dishes (>20% reduction; Figure 3f; q_{lac,counts} available in Supporting Information: Figure S4D), suggesting a higher rate of aerobic glycolysis in static cultures. The q_{lac} values decreased after 4 days of culture in both bioreactors and dish cultures to the same extent, which may be due to the concurrent reduction in growth rate. In addition to lactate, ammonia is a common inhibitor of cell proliferation. The ammonia production, however, was similar in bioreactor runs at 10% or 40% dO₂ and in standard dish cultures (Supporting Information: Figure S4B,E).

Although a 10% dO₂ setpoint is closer to the physiological oxygen concentrations in which erythroblasts proliferate in vivo, we conclude that the lower dO₂ does not alter growth or spontaneous differentiation compared to a 40% dO₂ setpoint.

3.4 | Shear stress affects erythroblast proliferation during expansion cultures

Shear stress is another critical parameter in mammalian cell cultures. It can have a negative effect on growth and viability (Neunstoecklin

et al., 2015), whereas insufficient stirring speeds leads to inadequate mixing and aeration when scaling up (Xing et al., 2009). To evaluate the effect of stirring speed on erythroblast proliferation, erythroblasts were inoculated in 0.5 L bioreactors, and the impeller speed was increased from 200 to 600 rpm (tip speed = 880 mm/s) and 1800 rpm (tip speed = 2640 mm/s). After 6 days of culture, a 87.2 ± 2.7-FC in cell number was observed in the 600 rpm cultivations (Figure 4a), similar to the growth levels previously observed at 200 rpm and in static cultures. By contrast, an agitation speed of 1800 rpm reduced proliferation during the first 4 days of culture, which, however, recovered to values comparable to those observed at 600 rpm after 6 days of culture (Figure 4b).

The increase in stirring speed to 600 rpm did not enhance spontaneous differentiation, with only 12.1 ± 2.8% cells in the most differentiated CD235⁺ CD49d⁻ compartment at Day 6. At 1800 rpm, however, CD49d expression decreased in the first 3 days of culture, stabilizing in the following days (Figure 4c). Cell cycle progression was not affected by the stirring speed (Supporting Information: Figure S5).

3.5 | Terminal differentiation of erythroblast cultures in bioreactors

We validated that erythroblasts expanded in bioreactors could be differentiated as standard static cultures throughout all conditions (data not shown). To examine terminal differentiation in bioreactors, Day 10 PBMC-derived erythroblast cultures were seeded in differentiation medium at a starting cell concentration of 1.5 × 10⁶ cells/ml, both in bioreactors and culture dishes (Figure 5a). Bioreactors were controlled with the same conditions as in the reference expansion phase (40% dO₂, pH 7.5, 200 rpm, 37°C). During the first 3 days of differentiation, cell numbers increased in both systems. Simultaneously, sparging was required to maintain dO₂ at 40% (Supporting Information: Figure S6). This was followed by a cell cycle arrest in both static and bioreactor conditions. Bioreactor cultures showed a gradual decrease in cell numbers until the end of culture, while cell numbers in static conditions remained similar (Figure 5b). Concurrently, the dO₂

FIGURE 3 Low dissolved oxygen (dO₂) concentration support erythroblast expansion. Erythroblasts were expanded from PBMCs for 9 days, and subsequently seeded in culture dishes (orange line) or STRs (100 ml/min N₂ headspace flow) at a starting cell concentration of 0.7 × 10⁶ cells/ml. dO₂ was controlled by air sparging when below the targeted setpoint (10% [purple line] or 40% [blue line], equivalent to 0.72 and 2.88 mg O₂/L, respectively), and by stripping of excess oxygen using 100 ml/min N₂ headspace flow. (a) Cell concentration monitored for 8 days of culture, with medium refreshment when the measured cell concentration (daily) was >1.2 × 10⁶ cells/ml. Fold change (FC) in cell number was calculated using the number of erythroblasts at the start of culture. (b) Growth rate was calculated for each day using the total biomass concentration (μm³ of total cell volume per ml of culture) assuming exponential growth between consecutive media refreshment events. (c) Mean cell diameter was measured daily. (d) and (e) Cells were stained with CD235a plus CD71 (d), or CD235a plus CD49d (e). (f) Cell-specific lactate production rate (q_{lac,vol}) calculated using growth rate data and measured extracellular lactate concentrations (see Supporting Information: Methods). All data are displayed as mean ± SD (error bars; n = 3 reactor runs/donors, unless indicated otherwise). Significance is shown for the comparison with dish cultures (unpaired two-tailed two-sample equal-variance Student's t-test; *p < 0.05, **p < 0.01, ***p < 0.001, not displayed if difference is not significant). Growth rates and q_{lac} calculated using cell counts available in Supporting Information: Figure S4. PBMC, peripheral blood mononuclear cell; STR, stirred tank reactor.

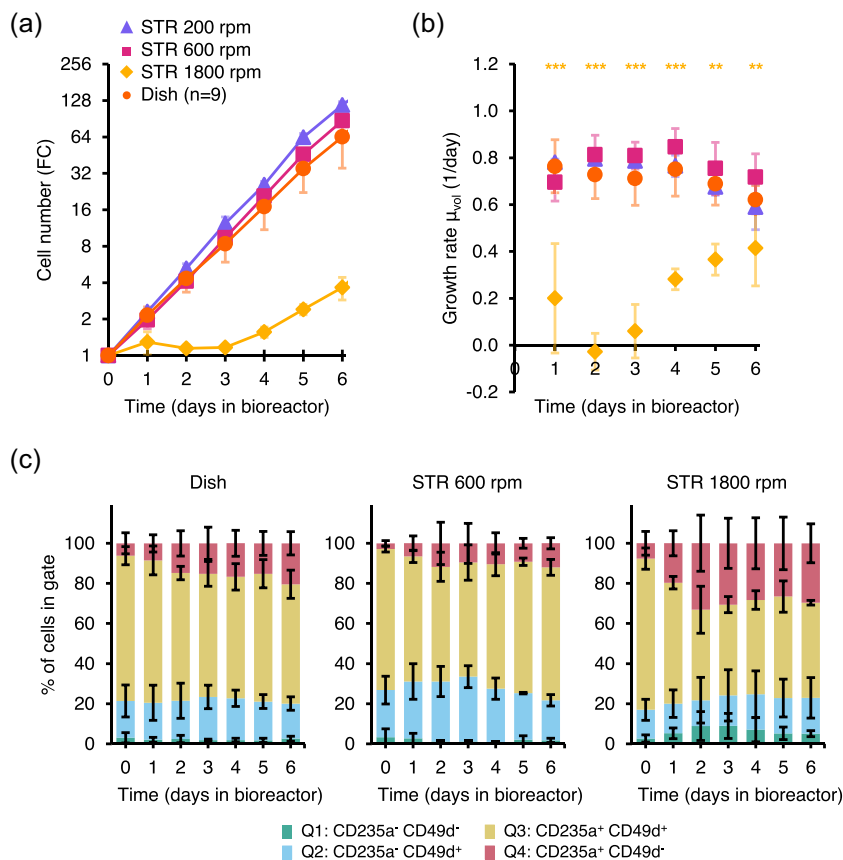


FIGURE 4 High stirring speeds can sustain erythroblast expansion. Erythroblasts were expanded from PBMCs for 9 days, and subsequently seeded in culture dishes (orange line) or STRs (dO₂: 40% controlled by sparging of air; 100 ml/min N₂ headspace flow) at a starting cell concentration of 0.7×10^6 cells/ml, under agitation at 200 (blue line), 600 (purple line), or 1800 rpm (yellow line). (a) Cells were maintained between 0.7 and 1.5×10^6 cells/ml by dilution with fresh medium. Cumulative cell numbers were calculated and represented as fold change (FC) compared to the start of the experiment. (b) Growth rate for each day was calculated assuming exponential growth between consecutive media refreshment events. (c) Cells were stained with CD235a plus CD49d to evaluate the progression of spontaneous differentiation during culture. All data are displayed as mean \pm SD (error bars; $n = 3$ reactor runs/donors, unless indicated otherwise). Significance is shown for the comparison with dish cultures (unpaired two-tailed two-sample equal-variance Student's *t*-test; ** $p < 0.01$, *** $p < 0.001$, not displayed if difference is not significant). PBMC, peripheral blood mononuclear cell. dO₂, dissolved oxygen; PBMC, peripheral blood mononuclear cell; STR, stirred tank reactor.

concentration increased in absence of sparging after 4 days of culture. A similar decrease in cell numbers was also observed for differentiating erythroblasts subjected to orbital shaking compared to static controls (manuscript in preparation). Here, the decrease was shown to originate from a disintegration of stiff pyrenocytes, whereas the number of enucleated and more flexible reticulocytes remained constant.

Differentiation was evident from a decrease in mean cell diameter in bioreactors and culture dishes (Figure 5c) with a concomitant loss of CD49d and CD71 expression (Figure 5d,e). Hemoglobin accumulation and enucleation efficiency was also similar in static and stirred bioreactors (Figure 5f,g). Presence of enucleated cells and egressed nuclei was confirmed by cytopins (Figure 5h). In conclusion, erythroblast differentiation could also be supported in our stirred bioreactor systems, reaching similar levels of enucleation to those of culture dishes, albeit with slightly lower cell yields.

3.6 | Expansion cultures can be scaled up to 3 L bioreactors

Knowing the boundaries to cultured erythroblast in STRs enabled us to scale-up from 300 ml cultures in 500 ml STRs to larger volumes. Day 8 erythroblasts cultures from PBMCs were seeded at a density of 0.7×10^6 cells/ml in a 500 ml STR (initial culture volume = 100–150 ml), and cell density was adjusted daily to 0.7×10^6 cells/ml by adding more medium. When the volume surpassed 400 ml, cells were transferred to a 3 L STR (minimum working volume = 800 ml), operated with a tip speed similar to that tested in 0.5 L bioreactors (300 mm/s; single down-pumping marine impeller; diameter = 5 cm; 115 rpm). Medium was added to maintain cell density until a total volume of 2.5 L was reached. Subsequently, the total volume was maintained at 2.5 L and excess cells were removed (Figure 6a,b). The cell cultures proliferated exponentially for 9 subsequent days achieving an average 196-fold increase in the 3 L STR, and 234-fold

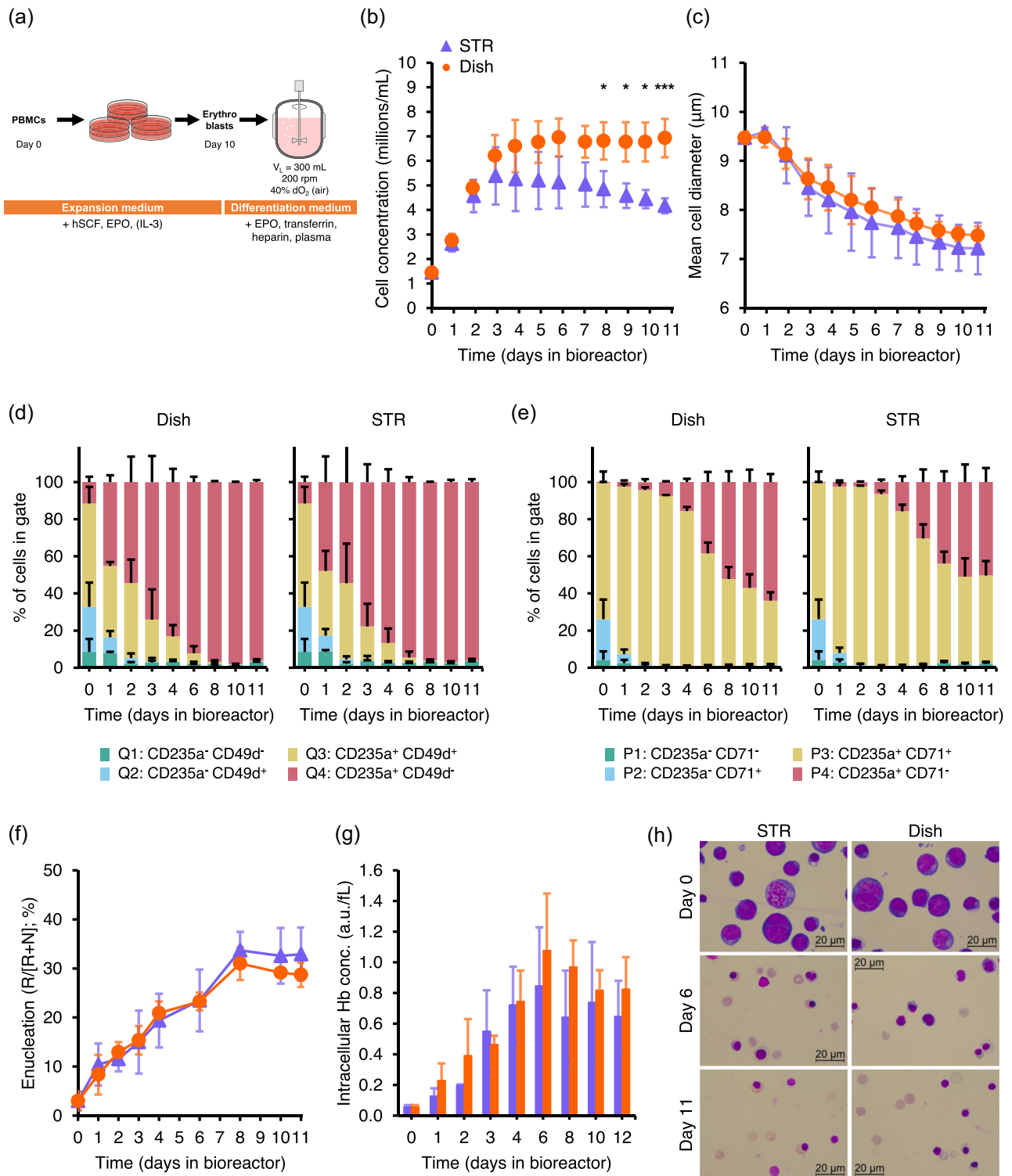


FIGURE 5 (See caption on next page)

under static conditions (Figure 6c). Interestingly, the variation between three cultures was smaller in the STR (range: 112–280-fold) compared to the same cultures expanded in dishes (range: 51–462-fold). After 9 days of culture, there was no difference in viability or differentiation stage of the cells (Figure 6d,e; Supporting Information: Figure S7A). Similar to the 300 ml cultures, lactate production in 2.5 L STRs was lower compared to static conditions (Supporting Information: Figure S7B).

4 | DISCUSSION

Efficient cRBC production requires the transition from static culture systems to scalable cultivation platforms. We established the process conditions (oxygen and agitation) required for effective expansion and differentiation of erythroblast cultures in STRs. Oxygen availability was critical during expansion of erythroblast cultures, whereas the requirement for oxygen decreased during terminal differentiation. Stirring speeds required for a homogeneous distribution of cells in the bioreactor did not affect cell growth or differentiation. Only much elevated stirring speeds led to a temporary cell growth arrest and an acceleration in spontaneous erythroblast differentiation. Within the operating boundaries established in this study, the STR culture volume could be scaled up from 300 to 2500 ml. Whereas static cultures show some variation in their expansion potential, STR cultures proved to be more reproducible, which adds to the reliability of the process.

4.1 | Oxygen requirements of erythroblast in culture

Using a combination of headspace N₂ gas flow and intermittent air allowed us to tightly control dO₂ in our bioreactor cultures. While low dO₂ setpoints can reduce the overall sparging requirements of the culture and are closer to the *in vivo* hematopoietic niche, no significant improvement on growth, lactate accumulation or spontaneous differentiation was observed in our experiments when the dO₂ setpoint was decreased from 40% to 10%. Although oxygen concentration setpoints lower than 10% dO₂ may enhance proliferation, maintaining a constant dO₂ < 10% in our set-up is technically

challenging due to the noise in dO₂ readings and the oscillations caused by the discrete sparging events. This could be addressed by using oxygen probes with lower response times or with aeration strategies in which gas composition is adjusted based on the dO₂ measurements, avoiding large oxygen concentration peaks during sparging. Studying the effect of lower and fluctuating dO₂ concentrations can provide further information on the potential challenges that could be faced in the large bioreactors required for the production of the required number of cRBCs for a single transfusion unit, in which oxygen and nutrient gradients are difficult to avoid, and the risk of having oxygen-limited regions is higher (Anane et al., 2021; Serrato et al., 2004).

The oxygen requirements of erythroblasts decreased during culture, from 2.01 to 0.55 pg/cell/h, and increasingly less during terminal differentiation. These values explain the fast decrease in dO₂ concentration in the initial 2 L bioreactor experiments, in which the k_{1a} (0.27 1/h; headspace aeration only) could only support theoretical early erythroblast concentrations of <0.97 × 10⁶ cells/ml. Seahorse assays, used to quantify glycolysis and mitochondrial OXPHOS of cells by measuring oxygen consumption rates and extracellular acidization rates, have been reported for cultured erythroblasts. However, these assays are performed with low cell numbers and using medium with a composition different to that used for culture, potentially resulting in q_{O₂} values not representative of the culture conditions (van der Windt et al., 2016). Bayley et al. (2017) reported much lower q_{O₂} values for their bioreactor cultures, decreasing from 0.063 pg/cell/h for early erythroblasts to 0.017 pg/cell/h in the later stages of differentiation. A similar decrease in oxygen requirements during erythroid differentiation was described by Browne et al. (2014), from 2.84 to 0.13 pg/cell/h for proerythroblasts and reticulocytes, respectively. This decrease in oxygen requirement could be a result of mitophagy at terminal stages of erythroblast differentiation decreasing mitochondria numbers and marking the shift to anaerobic metabolism as occurring in RBCs (Barde et al., 2013; M. Chen et al., 2008; Sandoval et al., 2008). Differences between our measured q_{O₂} values and those previously reported could be explained by differences in the differentiation status of erythroid cells used at the start of the bioreactor cultures, culture medium composition, or oxygen concentration (Moradi et al., 2021). Of note, our values are in agreement with measured oxygen uptake rates of other human cell lines (0.4–6.2 pg O₂/cell/h; Wagner

FIGURE 5 Erythroblast differentiation can be achieved in stirred tank bioreactors. Erythroblasts were expanded from PBMCs for 10 days, and subsequently seeded in differentiation medium at a starting cell concentration of 1 × 10⁶ cells/ml. (a) Cells were transferred to culture dishes or STRs and kept in culture for 11 subsequent days without medium refreshment. (b) Cell concentration during 11 days of differentiation in STRs (blue symbols) and dishes (orange symbols). (c) Mean cell diameter was measured daily. (d) and (e) Cells were stained with CD235a plus CD49d (d), or CD235a plus CD71 (e), and percentages in each quadrant are shown. (f) Enucleation percentage of erythroid cells was calculated from the forward scatter and DRAQ5 staining. DRAQ5⁻ cell numbers (reticulocytes, R) were divided by the sum of small DRAQ5⁺ events (nuclei, N + reticulocytes, R). (g) Hemoglobin was measured in arbitrary units (a.u.) and the intracellular hemoglobin concentration was calculated using the total cell volume. (h) Representative cytospin cell morphology by May–Grünwald–Giemsa (Pappenheim) staining of bioreactor cultures during differentiation. All data are displayed as mean ± SD (error bars; n = 3 reactor runs/donors). Significance is shown for the comparison with dish cultures (unpaired two-tailed two-sample equal-variance Student's *t*-test; **p* < 0.05, ****p* < 0.001, not displayed if difference is not significant). PBMC, peripheral blood mononuclear cell; STR, stirred tank reactor.

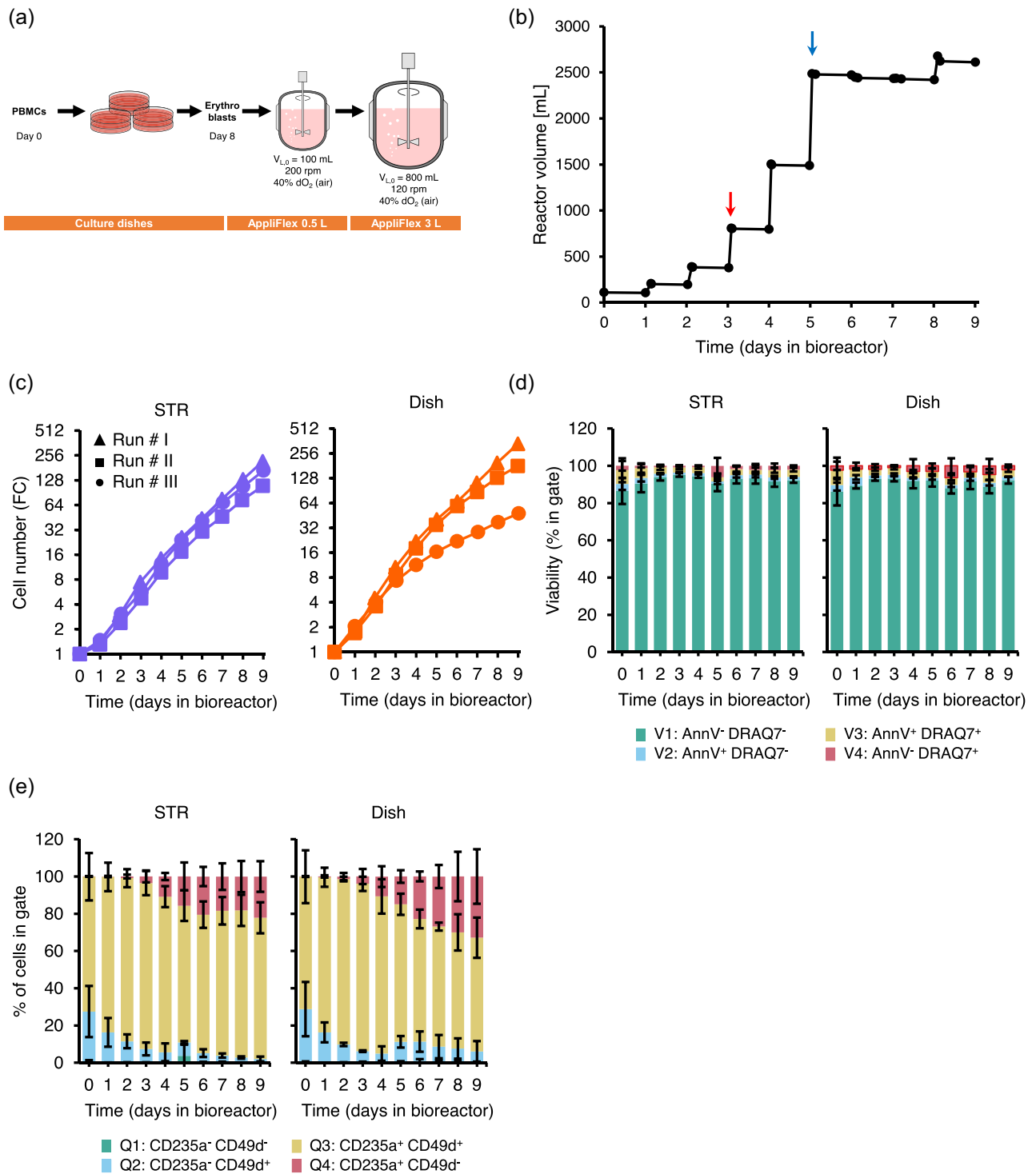


FIGURE 6 (See caption on next page)

et al., 2011). We suggest using continuous dO_2 measurements and the dynamic method to estimate qO_2 in erythroid cultures, as other methods such as using offgas data are difficult to implement due to the low oxygen consumption rates of mammalian cell cultures (Singh, 1996).

In this study, we used (intermittent) air sparging, together with a constant headspace nitrogen gas flow to enable a fast control of dO_2 and pH levels. Although the constant nitrogen flow leads to stripping of oxygen from the liquid, which was compensated by additional sparging, cell growth was similar to that observed in the reference static cultures in dishes. Furthermore, this strategy did not lead to significant foaming in the 0.5 L nor the 3 L bioreactor cultures (note that the medium has a low protein content; 0.1% w/w of albumin). This strategy can probably be applied for larger bioreactor cultures as well, especially when enriching the aeration with pure oxygen (Varley et al., 2004). Although dissolved CO_2 levels in bioreactor cultures ($pCO_2 = 10\text{--}40$ mmHg; data not shown) were similar to those under physiological conditions, CO_2 accumulation may represent a challenge for further scale up or at higher cell density cultures, for which CO_2 stripping via sparging will become more relevant (Pattison et al., 2000; Xing et al., 2017).

Foaming due to excessive sparging can negatively affect the process' performance by aggregation of expensive growth factors and other proteins in the foam layer (Walls et al., 2017; Xiao & Konermann, 2015), and an increased risk for the sterility of the process during a putative foam-out event (Vardar-Sukan, 1992). In case significant foaming appears, antifoams could be applied. Nevertheless, care has to be taken as there are reports that these reagents negatively affect mass transfer and cell growth (Al-Masry, 1999; Routledge et al., 2014; Velugula-Yellela et al., 2018). For example, pluronic F68, a nonsilicone-based copolymer antifoaming agent, reduces attachment of cells to rising gas bubbles, minimizing their exposure to bubble bursting (Chattopadhyay et al., 1995; Jordan et al., 1994; Ma et al., 2004; Tharmalingam et al., 2008). However, effects of pluronics on cell strength and stiffness, cell aggregation, and membrane trafficking processes have been described previously (Guzniczak et al., 2018; Sahay et al., 2008; Tharmalingam et al., 2008; Z. Zhang et al., 1992). For erythroid cultures, pluronics can reduce enucleation efficiency and potentially increase RBC aggregation (Armstrong et al., 2001; Bayley et al., 2017). Other antifoam agents

such as those based on silicone polymers can be problematic, as they can negatively affect equipment, decrease the efficiency of downstream steps, and have a toxic effect upon injection in patients (Harington, 1961; McGregor et al., 1988).

Antifoam addition has minimal effects on protecting cells to high gas entrance velocities, a major contributor of sparging-induced shear (Chaudhary et al., 2020; Zhu et al., 2008). Thus, we suggest the usage of spargers with larger pore sizes for larger scale bioreactor erythroid cultures to reduce the impact of high shear caused by bubble formation and detachment from the sparger. Even more promising is to replace sparging by a membrane gas exchanger, although cells could be exposed to new shear due to the continuous recirculation through the system. Furthermore the cultivation system gets much more complex and the cost of the process increases (Wang et al., 2017).

4.2 | Erythroid expansion cultures are robust to high stirring speeds

This study shows that erythroblast expansion cultures can withstand agitation speeds of up to 600 rpm (tip speed = 880 mm/s), without negatively affecting growth, viability, or the differentiation stage of the cells. Surprisingly, very high stirring speeds (1800 rpm) led to a temporary arrest in growth, followed by a recovery after 5–6 days, accompanied by an acceleration in erythroid differentiation as reported previously for erythroid cultures in flasks under orbital shaking (Aglialoro et al., 2021). This recovery in growth could be explained by an adaptation of culture cells to these turbulent conditions, or by the selection of erythroblast cells more tolerant to agitation during the first days of culture. A more thorough characterization of this adaptation on not only the erythroblast transcriptome but also at the lipidomic and metabolomic level will need to be performed to identify (signaling) pathways triggered by this mechanical stress, the nature of the adaptative response (e.g., membrane composition remodeling), and to determine the mechanism under which erythroid differentiation is promoted under these conditions.

Interestingly, other studies have reported less tolerance of erythroblast cultures to agitation. Increased apoptosis, acceleration

FIGURE 6 Scale-up of erythroblast expansion to 3 L stirred tank bioreactors. Erythroblasts were expanded from PBMCs for 8 days, and subsequently seeded in culture dishes or 0.5 L stirred tank bioreactors (starting volume: 100–200 ml) at a starting cell concentration of 0.7×10^6 cells/ml. (a) Cells were kept in culture following a fed batch feeding strategy in which medium was refreshed if the measured cell concentration (daily) was $>1.2 \times 10^6$ cells/ml. Upon reaching a total number of >400 million cells, the culture was transferred to a 3.0 L bioreactor (starting volume: 800 ml; 115 rpm with marine down-pumping impeller, diameter: 5.0 cm), which was progressively filled by daily medium additions. (b) Culture volume in the bioreactor for an exemplary run. Transition from the 0.5 L to the 3 L reactor was performed at Day 3 of culture (red arrow). Upon filling of the 3 L reactor (blue arrow), excess cells were harvested daily to keep a working volume of 2.5–2.7 L. (c) Erythroblast cell concentration was monitored for 9 days of culture. Fold change (FC) in cell number was calculated relative to erythroblast numbers at the start of culture. The same preculture was seeded in parallel in the STR and in a dish. (d) and (e) Cells were stained with AnnexinV (apoptosis staining) and DRAQ7 (cell impermeable DNA stain) (d), or CD235a plus CD49d (erythroid differentiation markers). Percentage of cells in each quadrant is included. (e) All data are displayed as mean \pm SD (error bars; $n = 3$ reactor runs/donors). PBMC, peripheral blood mononuclear cell; STR, stirred tank reactor.

of erythroid differentiation, and lower enucleation levels have been observed in a gyro-rocker bioreactor at low orbital speeds (20 rpm) (Boehm et al., 2010). Bayley et al. (2017) also observed a decrease in proliferation in stirred bioreactors compared to static cultures, although no significance difference on growth was observed between stirring speeds of 300 and 450 rpm (tip speeds = 180 and 270 mm/s, respectively). Han et al. (2021) observed a dependence on the inoculum age to agitation tolerance, with proerythroblast and basophilic erythroblast cultures showing a quick decrease in growth and viability in microbioreactors agitated at 300 rpm (tip speed = 180 mm/s), while more mature cells (Day 12 after CD34⁺ isolation and start of culture), could tolerate the same conditions. However, it is difficult to directly compare the hydrodynamic conditions between these reports, partly due to differences in the culture set-up but also due to a lack of consensus on which mixing parameter (rpm, tip speed, volumetric power input) is more appropriate to do this comparison, which together codefine the dynamic shear stress experienced by cells. Local turbulent energy dissipation rate (EDR) has been suggested as an alternative parameter to define optimal ranges of agitation for mammalian cell culture (Chalmers, 2015). Supporting the relevance of EDR, it has been recently reported that turbulence and not shear stress is critical for large scale platelet production (Ito et al., 2018). Estimates of EDR in STRs could be useful to rationally drive the scale-up of the process, ensuring limited exposure of erythroblast to excessive hydrodynamic forces.

Although the effect of shear stress and EDR can be evaluated in STRs by varying the agitation rate, changes in stirring speed also affect the mass transfer rate between the gas and liquid phases, impacting the aeration requirements to control dO₂ and pH at the defined setpoints. This, in turn, can influence the exposure of cells to high local O₂ (and CO₂, if pH is controlled with this gas) concentrations and to high EDR regions due to bubble bursting phenomena (Walls et al., 2017). A full uncoupling of agitation and aeration is challenging, as other aeration strategies such as using submerged oxygen-permeable membranes, can also lead to undesired effect such as very high local O₂ concentrations (Aunins & Henzler, 2001; Côté et al., 1989; Emery et al., 1995).

4.3 | Quantification of metabolite consumption/production rates in erythroid cultures

We observed a decrease in erythroblast proliferation during expansion cultures, with growth rates as low as ~0.3 1/day at the end of the cultures. Growth limitations in erythroblast batch and fed-batch cultures has been previously reported, but the origin of this limitation has not been identified yet (Bayley et al., 2017; Glen et al., 2018). Here, we report lactate and ammonium concentrations below 6 and 0.6 mM, respectively, which are lower than typical growth-inhibiting concentrations for other animal cell lines (Cruz et al., 2000; Hassell et al., 1991; Ozturk et al., 1992). Interestingly, we measured lactate production rates (q_{lac}) of 0.5–2.5 pmol/cell/day, significantly lower than those reported for other erythroid cultures (3–12 pmol/cell/day;

Bayley et al., 2017; Lee et al., 2018; Patel et al., 2000; Sivalingam et al., 2020). dO₂ concentration in the bioreactor did not have a significant effect on q_{lac} , but static cultures consistently showed higher rates in later days of culture. Oxygen limitations caused by low oxygen concentrations (<10% dO₂) in the bottom of culture dishes could lead to an increase in anaerobic glycolysis rates in erythroblasts cultured under static conditions, leading to the observed lactate production (Al-Ani et al., 2018). Even at the measured low concentrations, lactate can potentially induce activation of erythroid-related genes such as STAT5, affecting erythroid differentiation dynamics (Luo et al., 2017). Strategies to limit lactate production in culture could be implemented, such as feeding profiles that limit glucose concentrations during culture.

4.4 | Outlook

A 200-fold expansion per PBMC already takes place in the first 8 days of culture (before reactor inoculation), still performed under static conditions in culture dishes (Heshusius et al., 2019), resulting in an overall 200 × 750 = 150,000-fold expansion after 10 days of culture in the bioreactor. The high cell yields in this first culture stage are partly due to the positive contribution of CD14⁺ monocytes/macrophages present in the PBMC pool by the production of soluble factors that support erythroblast expansion (Heideveld et al., 2015; van den Akker et al., 2010). Full translation of our protocol to STRs would require defining operating conditions that would support proliferation and survival of HSC and macrophages in the first days of culture.

While we could scale-up erythroblast expansion cultures from dishes to 0.5 L and 3.0 L bioreactors, the large number of cells required for a single cRBC transfusion unit would still require prohibitively large STRs. Perfusion approaches can be used to increase cell concentrations, leading to a significant footprint reduction compared to fed-batch processes, and potentially to a lower production cost if the perfusion rate and perfusion media composition is sufficiently optimized (Pollock et al., 2013; Xu et al., 2017). Perfusion processes also support a more stable culture environment and cell metabolism, by continuously removing inhibitory metabolic byproducts (e.g., lactate and ammonia) and ensuring sufficient nutrient levels during culture (Walther et al., 2019; Zamani et al., 2018). The cell-retention strategies required for perfusion could also be of value to perform the required medium changes when transitioning from proliferation to differentiation in culture, where removal of hSCF and dexamethasone is needed for efficient maturation and enucleation. We expect our quantitative physiological data and observations on the effect of bioreactor operating parameters to be relevant for the further scale-up of erythroblast proliferation and differentiation bioreactor cultures, and the optimization of feeding regimes with the aim to achieve a cost-effective cRBC production process.

AUTHOR CONTRIBUTIONS

Joan Sebastián Gallego-Murillo performed the experiments. Joan Sebastián Gallego-Murillo, Emile van den Akker, Sebastian Aljoscha

Wahl, and Marieke von Lindern designed the experiments, analyzed the data, and wrote the manuscript. Giulia Iacono and Luuk A. M. van der Wielen contributed to data analysis and writing of the manuscript. All authors critically revised the manuscript.

ACKNOWLEDGMENTS

We thank Queralt Farras Costa and Victur Puig I Laborda (Department of Biotechnology, Faculty of Applied Sciences, Delft University of Technology; Delft; The Netherlands) for their assistance on the determination of oxygen consumption rates. We also thank Yi Song, Dirk Geerts and Rob Kerste (Department of Biotechnology, Faculty of Applied Sciences, Delft University of Technology; Delft; The Netherlands) for their support on setting up the 0.5 L bioreactors. We thank Nurcan Yagci (Sanquin Research) who performed PBMC isolation and precultures. We thank Marten Hansen (Laboratory for Cell Therapies, Sanquin) for the support on setting up the 3 L bioreactors. We thank Tom van Arragon and Cristina Bernal Martínez (Applikon Biotechnology; Delft; The Netherlands) for technical help and advice on bioreactor cultures in the Applikon systems. This study was supported by the ZonMW TAS program (project 116003004), by the Landsteiner Foundation for Bloodtransfusion Research (LSBR project 1239), by Sanquin Blood Supply grants PPOC17-28 and PPOC19-14, and by European Union, Marie Skłodowska-Curie Innovative Training Networks (860436; EVIDENCE).

CONFLICT OF INTEREST

The authors declare no conflict of interest.

DATA AVAILABILITY STATEMENT

The data that support the findings of this study are available from the corresponding author upon reasonable request.

NOMENCLATURE

μ_{\max}	Maximal growth rate (units = 1/day); can be calculated using cell counts ($\mu_{\max, \text{counts}}$) or biomass concentration ($\mu_{\max, \text{vol}}$).
τ	Doubling time (units = day).
C_{lac}	Extracellular lactate concentration (units: mol lactate/L).
C_N	Cell concentration (units: cells/ml of culture).
C_{NH_4}	Extracellular ammonium concentration (units: mol NH_4^+ /L).
C_{O_2}	Concentration of dissolved oxygen in the liquid (units: mg O_2 /L).
$C_{\text{O}_2}^{\text{sat}}$	Concentration of saturation for oxygen in the liquid (units: mg O_2 /L).
C_V	Biomass concentration (units: μm^3 of cells/ml of culture).
d_{O_2}	Dissolved oxygen concentration as percentage of the saturation concentration at the defined conditions (37°C, 1 atm, air; units = %).
$k_L a$	Overall volumetric mass transfer coefficient of the system for oxygen, recalculated to a liquid-side mass transfer oxygen composition gradient (units = 1/h).
N	Total number of cells (units: cells).

q_{lac}	Cell-specific production rate of lactate; can be calculated using cell counts ($q_{\text{lac, counts}}$; units = mol lactate/cell/day) or biomass concentration ($q_{\text{lac, volume}}$; units = mol lactate/ μm^3 cell/day).
q_{NH_4}	Cell-specific production rate of ammonium; can be calculated using cell counts ($q_{\text{NH}_4, \text{counts}}$; units = mol NH_4^+ /cell/day) or biomass concentration ($q_{\text{NH}_4, \text{volume}}$; units = mol NH_4^+ / μm^3 cell/day).
q_{O_2}	Cell-specific consumption rate of oxygen (units = pg O_2 /cell/day).
V_L	Volume of culture (units: L).

ORCID

Joan Sebastián Gallego-Murillo  <http://orcid.org/0000-0003-2381-2012>

REFERENCES

- Aglialoro, F., Abay, A., Yagci, N., Rab, M. A. E., Kaestner, L., van Wijk, R., von Lindern, M., & van den Akker, E. (2021). Mechanical stress induces Ca²⁺-dependent signal transduction in erythroblasts and modulates erythropoiesis. *International Journal of Molecular Sciences*, 22(2), 935. <https://doi.org/10.3390/ijms22020955>
- Aglialoro, F., Hofsink, N., Hofman, M., Brandhorst, N., & van den Akker, E. (2020). Inside out integrin activation mediated by PIEZO1 signaling in erythroblasts. *Frontiers in Physiology*, 11, 958. <https://doi.org/10.3389/fphys.2020.00958>
- Al-Ani, A., Toms, D., Kondro, D., Thundathil, J., Yu, Y., & Ungrin, M. (2018). Oxygenation in cell culture: Critical parameters for reproducibility are routinely not reported. *PLoS ONE*, 13(10), e0204269. <https://doi.org/10.1371/journal.pone.0204269>
- Allenby, M. C., Panoskaltzis, N., Tahlawi, A., Dos Santos, S. B., & Mantalaris, A. (2019). Dynamic human erythropoiesis in a three-dimensional perfusion bone marrow biomimicry. *Biomaterials*, 188, 24–37. <https://doi.org/10.1016/j.biomaterials.2018.08.020>
- Al-Masry, W. A. (1999). Effects of antifoam and scale-up on operation of bioreactors. *Chemical Engineering and Processing: Process Intensification*, 38(3), 197–201. [https://doi.org/10.1016/S0255-2701\(99\)00014-8](https://doi.org/10.1016/S0255-2701(99)00014-8)
- Anane, E., Knudsen, I. M., & Wilson, G. C. (2021). Scale-down cultivation in mammalian cell bioreactors—The effect of bioreactor mixing time on the response of CHO cells to dissolved oxygen gradients. *Biochemical Engineering Journal*, 166, 107870. <https://doi.org/10.1016/j.bej.2020.107870>
- Armstrong, J. K., Meiselman, H. J., Wenby, R. B., & Fisher, T. C. (2001). Modulation of red blood cell aggregation and blood viscosity by the covalent attachment of Pluronic copolymers. *Biorheology*, 38(2–3), 239–247.
- Aunins, J. G., & Henzler, H.-J. (2001). Aeration in cell culture bioreactors. In H.-J. Rehm, & G. Reed (Eds.), *Biotechnology set* (pp. 219–281). John Wiley & Sons Ltd. <https://doi.org/10.1002/9783527620999.ch11b>
- Avgerinos, G. C., Drapeau, D., Socolow, J. S., Mao, J., Hsiao, K., & Broeze, R. J. (1990). Spin filter perfusion system for high density cell culture: Production of recombinant urinary type plasminogen activator in CHO cells. *Bio/Technology*, 8(1), 54–58. <https://doi.org/10.1038/nbt0190-54>
- Bakker, W. J., Blázquez-Domingo, M., Kolbus, A., Besooyen, J., Steinlein, P., Beug, H., Coffey, P. J., Löwenberg, B., von Lindern, M., & van Dijk, T. B. (2004). FoxO3a regulates erythroid differentiation and induces BTG1, an activator of protein arginine methyl

- transferase 1. *Journal of Cell Biology*, 164(2), 175–184. <https://doi.org/10.1083/jcb.200307056>
- Bapat, A., Schippel, N., Shi, X., Jasbi, P., Gu, H., Kala, M., Sertil, A., & Sharma, S. (2021). Hypoxia promotes erythroid differentiation through the development of progenitors and proerythroblasts. *Experimental Hematology*, 97, 32–46. <https://doi.org/10.1016/j.exphem.2021.02.012>
- Barde, I., Rauwel, B., Marin-Florez, R. M., Corsinotti, A., Laurenti, E., Verp, S., Offner, S., Marquis, J., Kapopoulou, A., Vanicek, J., & Trono, D. (2013). A KRAB/KAP1-miRNA cascade regulates erythropoiesis through stage-specific control of mitophagy. *Science*, 340(6130), 350–353. <https://doi.org/10.1126/science.1232398>
- Bayley, R., Ahmed, F., Glen, K., McCall, M., Stacey, A., & Thomas, R. (2017). The productivity limit of manufacturing blood cell therapy in scalable stirred bioreactors. *Journal of Tissue Engineering and Regenerative Medicine*, 12, e368–e378. <https://doi.org/10.1002/term.2337>
- Boehm, D., Murphy, W. G., & Al-Rubeai, M. (2010). The effect of mild agitation on in vitro erythroid development. *Journal of Immunological Methods*, 360(1–2), 20–29. <https://doi.org/10.1016/j.jim.2010.05.007>
- Browne, S. M., Daud, H., Murphy, W. G., & Al-Rubeai, M. (2014). Measuring dissolved oxygen to track erythroid differentiation of hematopoietic progenitor cells in culture. *Journal of Biotechnology*, 187, 135–138. <https://doi.org/10.1016/j.jbiotec.2014.07.433>
- Brugarolas, J., Lei, K., Hurley, R. L., Manning, B. D., Reiling, J. H., Hafen, E., Witters, L. A., Ellisen, L. W., & Kaelin, W. G. (2004). Regulation of mTOR function in response to hypoxia by REDD1 and the TSC1/TSC2 tumor suppressor complex. *Genes & Development*, 18(23), 2893–2904. <https://doi.org/10.1101/gad.1256804>
- Caielli, S., Cardenas, J., de Jesus, A. A., Baisch, J., Walters, L., Blanck, J. P., Balasubramanian, P., Stagnar, C., Ohouo, M., Hong, S., Nassi, L., Stewart, K., Fuller, J., Gu, J., Banchemereau, J. F., Wright, T., Goldbach-Mansky, R., & Pascual, V. (2021). Erythroid mitochondrial retention triggers myeloid-dependent type I interferon in human SLE. *Cell*, 184(17), 4464–4479. <https://doi.org/10.1016/j.cell.2021.07.021>
- Caulier, A., Jankovsky, N., Demont, Y., Ouled-Haddou, H., Demagny, J., Guitton, C., Merlusca, L., Lebon, D., Vong, P., Aubry, A., Lahary, A., Rose, C., Gréaume, S., Cardon, E., Platon, J., Ouadid-Ahidouch, H., Rochette, J., Marolleau, J.-P., Picard, V., & Garçon, L. (2020). PIEZO1 activation delays erythroid differentiation of normal and hereditary xerocytosis-derived human progenitor cells. *Haematologica*, 105(3), 610–622. <https://doi.org/10.3324/haematol.2019.218503>
- Chalmers, J. J. (2015). Mixing, aeration and cell damage, 30+ years later: What we learned, how it affected the cell culture industry and what we would like to know more about. *Current Opinion in Chemical Engineering*, 10, 94–102. <https://doi.org/10.1016/j.coche.2015.09.005>
- Chattopadhyay, D., Rathman, J. F., & Chalmers, J. J. (1995). The protective effect of specific medium additives with respect to bubble rupture. *Biotechnology and Bioengineering*, 45(6), 473–480. <https://doi.org/10.1002/bit.260450603>
- Chaudhary, G., Luo, R., George, M., Tescione, L., Khetan, A., & Lin, H. (2020). Understanding the effect of high gas entrance velocity on Chinese hamster ovary (CHO) cell culture performance and its implications on bioreactor scale-up and sparger design. *Biotechnology and Bioengineering*, 117(6), 1684–1695. <https://doi.org/10.1002/bit.27314>
- Chen, K., Liu, J., Heck, S., Chasis, J. A., An, X., & Mohandas, N. (2009). Resolving the distinct stages in erythroid differentiation based on dynamic changes in membrane protein expression during erythropoiesis. *Proceedings of the National Academy of Sciences of the United States of America*, 106(41), 17413–17418. <https://doi.org/10.1073/pnas.0909296106>
- Chen, M., Sandoval, H., & Wang, J. (2008). Selective mitochondrial autophagy during erythroid maturation. *Autophagy*, 4(7), 926–928. <https://doi.org/10.4161/auto.6716>
- Chu, L., & Robinson, D. K. (2001). Industrial choices for protein production by large-scale cell culture. *Current Opinion in Biotechnology*, 12(2), 180–187. [https://doi.org/10.1016/S0958-1669\(00\)00197-X](https://doi.org/10.1016/S0958-1669(00)00197-X)
- Côté, P., Bersillon, J.-L., & Huyard, A. (1989). Bubble-free aeration using membranes: Mass transfer analysis. *Journal of Membrane Science*, 47(1), 91–106. [https://doi.org/10.1016/S0376-7388\(00\)80862-5](https://doi.org/10.1016/S0376-7388(00)80862-5)
- Cruz, H. J., Freitas, C. M., Alves, P. M., Moreira, J. L., & Carrondo, M. J. T. (2000). Effects of ammonia and lactate on growth, metabolism, and productivity of BHK cells. *Enzyme and Microbial Technology*, 27(1), 43–52. [https://doi.org/10.1016/S0141-0229\(00\)00151-4](https://doi.org/10.1016/S0141-0229(00)00151-4)
- Daniels, G. (2013). *Human blood groups* (3rd ed.). Wiley-Blackwell.
- Emery, A. N., Jan, D. C.-H., & Al-Rueai, M. (1995). Oxygenation of intensive cell-culture system. *Applied Microbiology and Biotechnology*, 43(6), 1028–1033. <https://doi.org/10.1007/BF00166920>
- Farid, S. S. (2007). Process economics of industrial monoclonal antibody manufacture. *Journal of Chromatography B: Analytical Technologies in the Biomedical and Life Sciences*, 848(1), 8–18. <https://doi.org/10.1016/j.jchromb.2006.07.037>
- Glen, K. E., Cheeseman, E. A., Stacey, A. J., & Thomas, R. J. (2018). A mechanistic model of erythroblast growth inhibition providing a framework for optimisation of cell therapy manufacturing. *Biochemical Engineering Journal*, 133, 28–38. <https://doi.org/10.1016/j.bej.2018.01.033>
- Godoy-Silva, R., Chalmers, J. J., Casnocha, S. A., Bass, L. A., & Ma, N. (2009). Physiological responses of CHO cells to repetitive hydrodynamic stress. *Biotechnology and Bioengineering*, 103(6), 1103–1117. <https://doi.org/10.1002/bit.22339>
- Gonzalez-Menendez, P., Romano, M., Yan, H., Deshmukh, R., Papoin, J., Oburoglu, L., Daumur, M., Dumé, A.-S., Phadke, I., Mongellaz, C., Qu, X., Bories, P.-N., Fontenay, M., An, X., Dardalhon, V., Sitbon, M., Zimmermann, V. S., Gallagher, P. G., Tardito, S., ... Kinet, S. (2021). An IDH1-vitamin C crosstalk drives human erythroid development by inhibiting pro-oxidant mitochondrial metabolism. *Cell Reports*, 34(5), 108723. <https://doi.org/10.1016/j.celrep.2021.108723>
- Goto, T., Ubukawa, K., Kobayashi, I., Sugawara, K., Asanuma, K., Sasaki, Y., Guo, Y.-M., Takahashi, N., Sawada, K., Wakui, H., & Nunomura, W. (2019). ATP produced by anaerobic glycolysis is essential for enucleation of human erythroblasts. *Experimental Hematology*, 72, 14–26. <https://doi.org/10.1016/j.exphem.2019.02.004>
- Griffiths, R. E., Kupzig, S., Cogan, N., Mankelov, T. J., Betin, V. M. S., Trakarsanga, K., Massey, E. J., Lane, J. D., Parsons, S. F., & Anstee, D. J. (2012). Maturing reticulocytes internalize plasma membrane in glycophorin A-containing vesicles that fuse with autophagosomes before exocytosis. *Blood*, 119(26), 6296–6306. <https://doi.org/10.1182/blood-2011-09-376475>
- Guzniczak, E., Jimenez, M., Irwin, M., Otto, O., Willoughby, N., & Bridle, H. (2018). Impact of poloxamer 188 (Pluronic F-68) additive on cell mechanical properties, quantification by real-time deformability cytometry. *Biomicrofluidics*, 12(4), 044118. <https://doi.org/10.1063/1.5040316>
- Han, S. Y., Lee, E. M., Lee, J., Lee, H., Kwon, A. M., Ryu, K. Y., Choi, W.-S., & Baek, E. J. (2021). Red cell manufacturing using parallel stirred-tank bioreactors at the final stages of differentiation enhances reticulocyte maturation. *Biotechnology and Bioengineering*, 118(5), 1763–1778. <https://doi.org/10.1002/bit.27691>
- Harington, J. S. (1961). A study of the chemical composition and potential hazards of an antifoam substance used in intracardiac surgery. *Thorax*, 16(2), 120–127.
- Hassell, T., Gleave, S., & Butler, M. (1991). Growth inhibition in animal cell culture. The effect of lactate and ammonia. *Applied Biochemistry and Biotechnology*, 30(1), 29–41. <https://doi.org/10.1007/BF02922022>

- Heideveld, E., Masiello, F., Marra, M., Esteghamat, F., Yağci, N., von Lindern, M., Migliaccio, A. R. F., & van den Akker, E. (2015). CD14+ cells from peripheral blood positively regulate hematopoietic stem and progenitor cell survival resulting in increased erythroid yield. *Haematologica*, 100(11), 1396–1406. <https://doi.org/10.3324/haematol.2015.125492>
- Heshusius, S., Heideveld, E., Burger, P., Thiel-Valkhof, M., Sellink, E., Varga, E., Ovchinnikova, E., Visser, A., Martens, J. H. A., von Lindern, M., & van den Akker, E. (2019). Large-scale in vitro production of red blood cells from human peripheral blood mononuclear cells. *Blood Advances*, 3(21), 3337–3350. <https://doi.org/10.1182/bloodadvances.2019000689>
- Housler, G. J., Miki, T., Schmelzer, E., Pekor, C., Zhang, X., Kang, L., Voskinarian-Berse, V., Abbot, S., Zeilinger, K., & Gerlach, J. C. (2012). Compartmental hollow fiber capillary membrane-based bioreactor technology for in vitro studies on red blood cell lineage direction of hematopoietic stem cells. *Tissue engineering. Part C, Methods*, 18(2), 133–142. <https://doi.org/10.1089/ten.TEC.2011.0305>
- Ito, Y., Nakamura, S., Sugimoto, N., Shigemori, T., Kato, Y., Ohno, M., Sakuma, S., Ito, K., Kumon, H., Hirose, H., Okamoto, H., Nogawa, M., Iwasaki, M., Kihara, S., Fujio, K., Matsumoto, T., Higashi, N., Hashimoto, K., Sawaguchi, A., ... Eto, K. (2018). Turbulence activates platelet biogenesis to enable clinical scale ex vivo production. *Cell*, 174(3), 636–648. <https://doi.org/10.1016/j.cell.2018.06.011>
- Jan, D. C. H., Petch, D. A., Huzel, N., & Butler, M. (1997). The effect of dissolved oxygen on the metabolic profile of a murine hybridoma grown in serum-free medium in continuous culture. *Biotechnology and Bioengineering*, 54(2), 153–164. [https://doi.org/10.1002/\(SICI\)1097-0290\(19970420\)54:2<153::AID-BIT7>3.0.CO;2-K](https://doi.org/10.1002/(SICI)1097-0290(19970420)54:2<153::AID-BIT7>3.0.CO;2-K)
- Jensen, E. L., Gonzalez-Ibanez, A. M., Mendoza, P., Ruiz, L. M., Riedel, C. A., Simon, F., Schuringa, J. J., & Elorza, A. A. (2019). Copper deficiency-induced anemia is caused by a mitochondrial metabolic reprogramming in erythropoietic cells. *Metallomics*, 11(2), 282–290. <https://doi.org/10.1039/c8mt00224j>
- Jordan, M., Eppenberger, H. M., Sucker, H., Widmer, F., & Einsele, A. (1994). Interactions between animal cells and gas bubbles: The influence of serum and pluronic F68 on the physical properties of the bubble surface. *Biotechnology and Bioengineering*, 43(6), 446–454. <https://doi.org/10.1002/bit.260430603>
- Karst, D. J., Serra, E., Villiger, T. K., Soos, M., & Morbidelli, M. (2016). Characterization and comparison of ATF and TFF in stirred bioreactors for continuous mammalian cell culture processes. *Biochemical Engineering Journal*, 110, 17–26. <https://doi.org/10.1016/j.bej.2016.02.003>
- Klinkenberg, E. F., Huis In't Veld, E. M. J., de Wit, P. D., van Dongen, A., Daams, J. G., de Kort, W. L. A. M., & Fransen, M. P. (2019). Blood donation barriers and facilitators of Sub-Saharan African migrants and minorities in Western high-income countries: A systematic review of the literature. *Transfusion Medicine*, 29(Suppl 1), 28–41. <https://doi.org/10.1111/tme.12517>
- Koleva, L., Bovt, E., Ataulkhanov, F., & Sinauridze, E. (2020). Erythrocytes as carriers: From drug delivery to biosensors. *Pharmaceutics*, 12(3), E276. <https://doi.org/10.3390/pharmaceutics12030276>
- Kretzmer, G., & Schügerl, K. (1991). Response of mammalian cells to shear stress. *Applied Microbiology and Biotechnology*, 34(5), 613–616. <https://doi.org/10.1007/BF00167909>
- Kupzig, S., Parsons, S. F., Curnow, E., Anstee, D. J., & Blair, A. (2017). Superior survival of ex vivo cultured human reticulocytes following transfusion into mice. *Haematologica*, 102(3), 476–483. <https://doi.org/10.3324/haematol.2016.154443>
- Leberbauer, C., Boulmé, F., Unfried, G., Huber, J., Beug, H., & Müllner, E. W. (2005). Different steroids co-regulate long-term expansion versus terminal differentiation in primary human erythroid progenitors. *Blood*, 105(1), 85–94. <https://doi.org/10.1182/blood-2004-03-1002>
- Lee, E., Han, S. Y., Choi, H. S., Chun, B., Hwang, B., & Baek, E. J. (2015). Red blood cell generation by three-dimensional aggregate cultivation of late erythroblasts. *Tissue Engineering. Part A*, 21(3–4), 817–828. <https://doi.org/10.1089/ten.tea.2014.0325>
- Lee, E., Lim, Z. R., Chen, H.-Y., Yang, B. X., Lam, A. T.-L., Chen, A. K.-L., Sivalingam, J., Reuveny, S., Loh, Y.-H., & Oh, S. K.-W. (2018). Defined serum-free medium for bioreactor culture of an immortalized human erythroblast cell line. *Biotechnology Journal*, 13(4), e1700567. <https://doi.org/10.1002/biot.201700567>
- Luo, S.-T., Zhang, D.-M., Qin, Q., Lu, L., Luo, M., Guo, F.-C., Shi, H.-S., Jiang, L., Shao, B., Li, M., Yang, H.-S., & Wei, Y.-Q. (2017). The promotion of erythropoiesis via the regulation of reactive oxygen species by lactic acid. *Scientific Reports*, 7, 38105. <https://doi.org/10.1038/srep38105>
- Ma, N., Chalmers, J. J., Auniņš, J. G., Zhou, W., & Xie, L. (2004). Quantitative studies of cell-bubble interactions and cell damage at different Pluronic F-68 and cell concentrations. *Biotechnology Progress*, 20(4), 1183–1191. <https://doi.org/10.1021/bp0342405>
- Mas-Bargues, C., Sanz-Ros, J., Román-Domínguez, A., Inglés, M., Gimeno-Mallench, L., El Alami, M., Viña-Almunia, J., Gambini, J., Viña, J., & Borrás, C. (2019). Relevance of oxygen concentration in stem cell culture for regenerative medicine. *International Journal of Molecular Sciences*, 20(5), 1195. <https://doi.org/10.3390/ijms20051195>
- McGregor, W. C., Weaver, J. F., & Tansey, S. P. (1988). Antifoam effects on ultrafiltration. *Biotechnology and Bioengineering*, 31(4), 385–389. <https://doi.org/10.1002/bit.260310416>
- Migliaccio, G., Di Pietro, R., di Giacomo, V., Di Baldassarre, A., Migliaccio, A. R., Maccioni, L., Galanello, R., & Papayannopoulou, T. (2002). In vitro mass production of human erythroid cells from the blood of normal donors and of thalassemic patients. *Blood Cells, Molecules, and Diseases*, 28(2), 169–180. <https://doi.org/10.1006/bcmd.2002.0502>
- Mohebbi-Kalhari, D., Behzadmehr, A., Doillon, C. J., & Hadjizadeh, A. (2012). Computational modeling of adherent cell growth in a hollow-fiber membrane bioreactor for large-scale 3-D bone tissue engineering. *Journal of Artificial Organs*, 15(3), 250–265. <https://doi.org/10.1007/s10047-012-0649-1>
- Moradi, F., Moffatt, C., & Stuart, J. A. (2021). The effect of oxygen and micronutrient composition of cell growth media on cancer cell bioenergetics and mitochondrial networks. *Biomolecules*, 11(8), 1177. <https://doi.org/10.3390/biom11081177>
- Murhammer, D. W., & Goochee, C. F. (1990). Sparged animal cell bioreactors: Mechanism of cell damage and Pluronic F-68 protection. *Biotechnology Progress*, 6(5), 391–397. <https://doi.org/10.1021/bp00005a012>
- Neunstoeklin, B., Stettler, M., Solacroup, T., Broly, H., Morbidelli, M., & Soos, M. (2015). Determination of the maximum operating range of hydrodynamic stress in mammalian cell culture. *Journal of Biotechnology*, 194, 100–109. <https://doi.org/10.1016/j.jbiotec.2014.12.003>
- Ozturk, S. S., & Palsson, B. O. (1991). Effect of medium osmolarity on hybridoma growth, metabolism, and antibody production. *Biotechnology and Bioengineering*, 37(10), 989–993. <https://doi.org/10.1002/bit.260371015>
- Ozturk, S. S., Riley, M. R., & Palsson, B. O. (1992). Effects of ammonia and lactate on hybridoma growth, metabolism, and antibody production. *Biotechnology and Bioengineering*, 39(4), 418–431. <https://doi.org/10.1002/bit.260390408>
- Patel, S. D., Papoutsakis, E. T., Winter, J. N., & Miller, W. M. (2000). The lactate issue revisited: Novel feeding protocols to examine inhibition of cell proliferation and glucose metabolism in hematopoietic cell

- cultures. *Biotechnology Progress*, 16(5), 885–892. <https://doi.org/10.1021/bp000080a>
- Pattison, R. N., Swamy, J., Mendenhall, B., Hwang, C., & Frohlich, B. T. (2000). Measurement and control of dissolved carbon dioxide in mammalian cell culture processes using an in situ fiber optic chemical sensor. *Biotechnology Progress*, 16(5), 769–774. <https://doi.org/10.1021/bp000089c>
- Pellegrin, S., Severn, C. E., & Toye, A. M. (2021). Towards manufactured red blood cells for the treatment of inherited anemia. *Haematologica*, 106, 2304–2311. <https://doi.org/10.3324/haematol.2020.268847>
- Peniche Silva, C. J., Liebsch, G., Meier, R. J., Gutbrod, M. S., Balmayor, E. R., & van Griensven, M. (2020). A new non-invasive technique for measuring 3D-oxygen gradients in wells during mammalian cell culture. *Frontiers in Bioengineering and Biotechnology*, 8, 595. <https://doi.org/10.3389/fbioe.2020.00595>
- Peyrard, T., Bardiaux, L., Krause, C., Kobari, L., Lapillonne, H., Andreu, G., & Douay, L. (2011). Banking of pluripotent adult stem cells as an unlimited source for red blood cell production: Potential applications for alloimmunized patients and rare blood challenges. *Transfusion Medicine Reviews*, 25(3), 206–216. <https://doi.org/10.1016/j.tmr.2011.01.002>
- Piret, J. M., Devens, D. A., & Cooney, C. L. (1991). Nutrient and metabolite gradients in mammalian cell hollow fiber bioreactors. *The Canadian Journal of Chemical Engineering*, 69(2), 421–428. <https://doi.org/10.1002/cjce.5450690204>
- Place, T. L., Domann, F. E., & Case, A. J. (2017). Limitations of oxygen delivery to cells in culture: An underappreciated problem in basic and translational research. *Free Radical Biology and Medicine*, 113, 311–322. <https://doi.org/10.1016/j.freeradbiomed.2017.10.003>
- Pollock, J., Ho, S. V., & Farid, S. S. (2013). Fed-batch and perfusion culture processes: Economic, environmental, and operational feasibility under uncertainty. *Biotechnology and Bioengineering*, 110(1), 206–219. <https://doi.org/10.1002/bit.24608>
- Preissmann, A., Wiesmann, R., Buchholz, R., Werner, R. G., & Noé, W. (1997). Investigations on oxygen limitations of adherent cells growing on macroporous microcarriers. *Cytotechnology*, 24(2), 121–134. <https://doi.org/10.1023/A:1007973924865>
- Ratcliffe, E., Glen, K. E., Workman, V. L., Stacey, A. J., & Thomas, R. J. (2012). A novel automated bioreactor for scalable process optimisation of haematopoietic stem cell culture. *Journal of Biotechnology*, 161(3), 387–390. <https://doi.org/10.1016/j.jbiotec.2012.06.025>
- Restelli, V., Wang, M.-D., Huzel, N., Ethier, M., Perreault, H., & Butler, M. (2006). The effect of dissolved oxygen on the production and the glycosylation profile of recombinant human erythropoietin produced from CHO cells. *Biotechnology and Bioengineering*, 94(3), 481–494. <https://doi.org/10.1002/bit.20875>
- Richard, A., Vallin, E., Romestaing, C., Roussel, D., Gandrillon, O., & Gonin-Giraud, S. (2019). Erythroid differentiation displays a peak of energy consumption concomitant with glycolytic metabolism rearrangements. *PLoS ONE*, 14(9), e0221472. <https://doi.org/10.1371/journal.pone.0221472>
- Rodrigues, M. E., Costa, A. R., Henriques, M., Azeredo, J., & Oliveira, R. (2010). Technological progresses in monoclonal antibody production systems. *Biotechnology Progress*, 26(2), 332–351. <https://doi.org/10.1002/btpr.348>
- Routledge, S. J., Poyner, D. R., & Bill, R. M. (2014). Antifoams: The overlooked additive? *Pharmaceutical Bioprocessing*, 2(2), 103–106. <https://doi.org/10.2217/PBP.14.5>
- Sahay, G., Batrakova, E. V., & Kabanov, A. V. (2008). Different internalization pathways of polymeric micelles and unimers and their effects on vesicular transport. *Bioconjugate Chemistry*, 19(10), 2023–2029. <https://doi.org/10.1021/bc8002315>
- Sandoval, H., Thiagarajan, P., Dasgupta, S. K., Schumacher, A., Prchal, J. T., Chen, M., & Wang, J. (2008). Essential role for Nix in autophagic maturation of erythroid cells. *Nature*, 454(7201), 232–235. <https://doi.org/10.1038/nature07006>
- Serrato, J. A., Palomares, L. A., Meneses-Acosta, A., & Ramírez, O. T. (2004). Heterogeneous conditions in dissolved oxygen affect N-glycosylation but not productivity of a monoclonal antibody in hybridoma cultures. *Biotechnology and Bioengineering*, 88(2), 176–188. <https://doi.org/10.1002/bit.20232>
- Severn, C. E., Eissa, A. M., Langford, C. R., Parker, A., Walker, M., Dobbe, J. G. G., Streekstra, G. J., Cameron, N. R., & Toye, A. M. (2019). Ex vivo culture of adult CD34⁺ stem cells using functional highly porous polymer scaffolds to establish biomimicry of the bone marrow niche. *Biomaterials*, 225, 119533. <https://doi.org/10.1016/j.biomaterials.2019.119533>
- Severn, C. E., Macedo, H., Eagle, M. J., Rooney, P., Mantalaris, A., & Toye, A. M. (2016). Polyurethane scaffolds seeded with CD34(+) cells maintain early stem cells whilst also facilitating prolonged egress of haematopoietic progenitors. *Scientific Reports*, 6, 32149. <https://doi.org/10.1038/srep32149>
- Sieblist, C., Jenzsch, M., & Pohlscheidt, M. (2016). Equipment characterization to mitigate risks during transfers of cell culture manufacturing processes. *Cytotechnology*, 68(4), 1381–1401. <https://doi.org/10.1007/s10616-015-9899-0>
- Singh, V. (1996). On-line measurement of oxygen uptake in cell culture using the dynamic method. *Biotechnology and Bioengineering*, 52(3), 443–448. [https://doi.org/10.1002/\(SICI\)1097-0290\(19961105\)52:3<443::AID-BIT12>3.0.CO;2-K](https://doi.org/10.1002/(SICI)1097-0290(19961105)52:3<443::AID-BIT12>3.0.CO;2-K)
- Sivalingam, J., SuE, Y., Lim, Z. R., Lam, A. T. L., Lee, A. P., Lim, H. L., Chen, H. Y., Tan, H. K., Warrier, T., Hang, J. W., Nazir, N. B., Tan, A. H. M., Renia, L., Loh, Y. H., Reuveny, S., Malleret, B., & Oh, S. K. W. (2020). A scalable suspension platform for generating high-density cultures of universal red blood cells from human induced pluripotent stem cells. *Stem Cell Reports*, 16(1), 182–197. <https://doi.org/10.1016/j.stemcr.2020.11.008>
- Sobolewski, P., Kandel, J., Klinger, A. L., & Eckmann, D. M. (2011). Air bubble contact with endothelial cells in vitro induces calcium influx and IP3-dependent release of calcium stores. *American Journal of Physiology—Cell Physiology*, 301(3), C679–C686. <https://doi.org/10.1152/ajpcell.00046.2011>
- Spencer, J. A., Ferraro, F., Roussakis, E., Klein, A., Wu, J., Runnels, J. M., Zaher, W., Mortensen, L. J., Alt, C., Turcotte, R., Yusuf, R., Côté, D., Vinogradov, S. A., Scadden, D. T., & Lin, C. P. (2014). Direct measurement of local oxygen concentration in the bone marrow of live animals. *Nature*, 508(7495), 269–273. <https://doi.org/10.1038/nature13034>
- Sugiura, S., Sakai, Y., Nakazawa, K., & Kanamori, T. (2011). Superior oxygen and glucose supply in perfusion cell cultures compared to static cell cultures demonstrated by simulations using the finite element method. *Biomicrofluidics*, 5(2), 022202. <https://doi.org/10.1063/1.3589910>
- Sun, X., Han, X., Xu, L., Gao, M., Xu, J., Yang, R., & Liu, Z. (2017). Surface-Engineering of red blood cells as artificial antigen presenting cells promising for cancer immunotherapy. *Small*, 13(40), 1701864. <https://doi.org/10.1002/sml.201701864>
- Tapia, F., Vázquez-Ramírez, D., Genzel, Y., & Reichl, U. (2016). Bioreactors for high cell density and continuous multi-stage cultivations: Options for process intensification in cell culture-based viral vaccine production. *Applied Microbiology and Biotechnology*, 100, 2121–2132. <https://doi.org/10.1007/s00253-015-7267-9>
- Tharmalingam, T., Ghebeh, H., Wuerz, T., & Butler, M. (2008). Pluronic enhances the robustness and reduces the cell attachment of mammalian cells. *Molecular Biotechnology*, 39(2), 167–177. <https://doi.org/10.1007/s12033-008-9045-8>
- Timmins, N. E., Athanasas, S., Günther, M., Buntine, P., & Nielsen, L. K. (2011). Ultra-high-yield manufacture of red blood cells from

- hematopoietic stem cells. *Tissue Engineering Part C: Methods*, 17(11), 1131–1137. <https://doi.org/10.1089/ten.tec.2011.0207>
- Timmins, N. E., & Nielsen, L. K. (2009). Blood cell manufacture: Current methods and future challenges. *Trends in Biotechnology*, 27(7), 415–422. <https://doi.org/10.1016/j.tibtech.2009.03.008>
- Timmins, N. E., & Nielsen, L. K. (2011). Manufactured RBC—Rivers of blood, or an oasis in the desert. *Biotechnology Advances*, 29(6), 661–666. <https://doi.org/10.1016/j.biotechadv.2011.05.002>
- Trakarsanga, K., Griffiths, R. E., Wilson, M. C., Blair, A., Satchwell, T. J., Meinders, M., Cogan, N., Kupzig, S., Kurita, R., Nakamura, Y., Toye, A. M., Anstee, D. J., & Frayne, J. (2017). An immortalized adult human erythroid line facilitates sustainable and scalable generation of functional red cells. *Nature Communications*, 8, 14750. <https://doi.org/10.1038/ncomms14750>
- van den Akker, E., Satchwell, T. J., Pellegrin, S., Daniels, G., & Toye, A. M. (2010). The majority of the in vitro erythroid expansion potential resides in CD34(−) cells, outweighing the contribution of CD34(+) cells and significantly increasing the erythroblast yield from peripheral blood samples. *Haematologica*, 95(9), 1594–1598. <https://doi.org/10.3324/haematol.2009.019828>
- van der Windt, G. J. W., Chang, C.-H., & Pearce, E. L. (2016). Measuring bioenergetics in T cells using a Seahorse extracellular flux analyzer. *Current Protocols in Immunology*, 113, 3.16B.1–3.16B.14. <https://doi.org/10.1002/0471142735.im0316bs113>
- Vardar-Sukan, F. (1992). Foaming and its control in bioprocesses. In F. Vardar-Sukan, & Ş. S. Sukan (Eds.), *Recent advances in biotechnology* (pp. 113–146). Springer. https://doi.org/10.1007/978-94-011-2468-3_6
- Varley, J., Brown, A. K., Boyd, J. W. R., Dodd, P. W., & Gallagher, S. (2004). Dynamic multi-point measurement of foam behaviour for a continuous fermentation over a range of key process variables. *Biochemical Engineering Journal*, 20(1), 61–72. <https://doi.org/10.1016/j.bej.2004.02.012>
- Velugula-Yellela, S. R., Williams, A., Trunfio, N., Hsu, C., Chavez, B., Yoon, S., & Agarabi, C. (2018). Impact of media and antifoam selection on monoclonal antibody production and quality using a high throughput micro-bioreactor system. *Biotechnology Progress*, 34(1), 262–270. <https://doi.org/10.1002/btpr.2575>
- Vichinsky, E. P., Earles, A., Johnson, R. A., Hoag, M. S., Williams, A., & Lubin, B. (1990). Alloimmunization in sickle cell anemia and transfusion of racially unmatched blood. *The New England Journal of Medicine*, 322(23), 1617–1621. <https://doi.org/10.1056/NEJM199006073222301>
- Villiger, T. K., Morbidelli, M., & Soos, M. (2015). Experimental determination of maximum effective hydrodynamic stress in multiphase flow using shear sensitive aggregates. *AIChE Journal*, 61(5), 1735–1744. <https://doi.org/10.1002/aic.14753>
- Vlaski, M., Lafarge, X., Chevaleyre, J., Duchez, P., Boiron, J.-M., & Ivanovic, Z. (2009). Low oxygen concentration as a general physiologic regulator of erythropoiesis beyond the EPO-related downstream tuning and a tool for the optimization of red blood cell production ex vivo. *Experimental Hematology*, 37(5), 573–584. <https://doi.org/10.1016/j.exphem.2009.01.007>
- von Lindern, M., Zauner, W., Mellitzer, G., Steinlein, P., Fritsch, G., Huber, K., Löwenberg, B., & Beug, H. (1999). The glucocorticoid receptor cooperates with the erythropoietin receptor and c-Kit to enhance and sustain proliferation of erythroid progenitors in vitro. *Blood*, 94(2), 550–559.
- Wagner, B. A., Venkataraman, S., & Buettner, G. R. (2011). The rate of oxygen utilization by cells. *Free Radical Biology & Medicine*, 51(3), 700–712. <https://doi.org/10.1016/j.freeradbiomed.2011.05.024>
- Walls, P. L. L., McRae, O., Natarajan, V., Johnson, C., Antoniou, C., & Bird, J. C. (2017). Quantifying the potential for bursting bubbles to damage suspended cells. *Scientific Reports*, 7(1), 1–9. <https://doi.org/10.1038/s41598-017-14531-5>
- Walsh, C., Ovenden, N., Stride, E., & Cheema, U. (2017). Quantification of cell-bubble interactions in a 3D engineered tissue phantom. *Scientific Reports*, 7(1), 6331. <https://doi.org/10.1038/s41598-017-06678-y>
- Walther, J., Lu, J., Hollenbach, M., Yu, M., Hwang, C., McLarty, J., & Brower, K. (2019). Perfusion cell culture decreases process and product heterogeneity in a head-to-head comparison with fed-batch. *Biotechnology Journal*, 14(2), 1700733. <https://doi.org/10.1002/biot.201700733>
- Wang, S., Godfrey, S., Ravikrishnan, J., Lin, H., Vogel, J., & Coffman, J. (2017). Shear contributions to cell culture performance and product recovery in ATF and TFF perfusion systems. *Journal of Biotechnology*, 246, 52–60. <https://doi.org/10.1016/j.jbiotec.2017.01.020>
- Wolfe, R. P., & Ahsan, T. (2013). Shear stress during early embryonic stem cell differentiation promotes hematopoietic and endothelial phenotypes. *Biotechnology and Bioengineering*, 110(4), 1231–1242. <https://doi.org/10.1002/bit.24782>
- World Health Organization. (2021). *Guidance on centralization of blood donation testing and processing*. <https://apps.who.int/iris/handle/10665/340182>
- Wu, S.-C. (1999). Influence of hydrodynamic shear stress on microcarrier-attached cell growth: Cell line dependency and surfactant protection. *Bioprocess Engineering*, 21(3), 201–206. <https://doi.org/10.1007/s004490050663>
- Xiao, Y., & Konermann, L. (2015). Protein structural dynamics at the gas/water interface examined by hydrogen exchange mass spectrometry. *Protein Science: A Publication of the Protein Society*, 24(8), 1247–1256. <https://doi.org/10.1002/pro.2680>
- Xing, Z., Kenty, B. M., Li, Z. J., & Lee, S. S. (2009). Scale-up analysis for a CHO cell culture process in large-scale bioreactors. *Biotechnology and Bioengineering*, 103(4), 733–746. <https://doi.org/10.1002/bit.22287>
- Xing, Z., Lewis, A. M., Borys, M. C., & Li, Z. J. (2017). A carbon dioxide stripping model for mammalian cell culture in manufacturing scale bioreactors. *Biotechnology and Bioengineering*, 114(6), 1184–1194. <https://doi.org/10.1002/bit.26232>
- Xu, S., Gavin, J., Jiang, R., & Chen, H. (2017). Bioreactor productivity and media cost comparison for different intensified cell culture processes. *Biotechnology Progress*, 33(4), 867–878. <https://doi.org/10.1002/btpr.2415>
- Yu, P. (2012). Numerical simulation on oxygen transfer in a porous scaffold for animal cell culture. *International Journal of Heat and Mass Transfer*, 55(15), 4043–4052. <https://doi.org/10.1016/j.ijheatmasstransfer.2012.03.046>
- Zamani, L., Lundqvist, M., Zhang, Y., Aberg, M., Edfors, F., Bidkhorji, G., Lindahl, A., Mie, A., Mardinoglu, A., Field, R., Turner, R., Rockberg, J., & Chotteau, V. (2018). High cell density perfusion culture has a maintained exoproteome and metabolome. *Biotechnology Journal*, 13, 1800036. <https://doi.org/10.1002/biot.201800036>
- Zhang, X., Luo, M., Dastagir, S. R., Nixon, M., Khamhoung, A., Schmidt, A., Lee, A., Subbiah, N., McLaughlin, D. C., Moore, C. L., Gribble, M., Bayhi, N., Amin, V., Pepi, R., Pawar, S., Lyford, T. J., Soman, V., Mellen, J., Carpenter, C. L., ... Chen, T. F. (2021). Engineered red blood cells as an off-the-shelf allogeneic anti-tumor therapeutic. *Nature Communications*, 12(1), 2637. <https://doi.org/10.1038/s41467-021-22898-3>
- Zhang, Y., Wang, C., Wang, L., Shen, B., Guan, X., Tian, J., Ren, Z., Ding, X., Ma, Y., Dai, W., & Jiang, Y. (2017). Large-scale ex vivo generation of human red blood cells from cord blood CD34⁺ cells. *Stem Cells Translational Medicine*, 6(8), 1698–1709. <https://doi.org/10.1002/sctm.17-0057>
- Zhang, Z., al-Rubeai, M., & Thomas, C. R. (1992). Effect of pluronic F-68 on the mechanical properties of mammalian cells. *Enzyme and Microbial Technology*, 14(12), 980–983. [https://doi.org/10.1016/0141-0229\(92\)90081-x](https://doi.org/10.1016/0141-0229(92)90081-x)

Zhu, Y., Cuenca, J. V., Zhou, W., & Varma, A. (2008). NSO cell damage by high gas velocity sparging in protein-free and cholesterol-free cultures. *Biotechnology and Bioengineering*, 101(4), 751–760. <https://doi.org/10.1002/bit.21950>

SUPPORTING INFORMATION

Additional supporting information can be found online in the Supporting Information section at the end of this article.

How to cite this article: Gallego-Murillo, J. S., Iacono, G., van der Wielen, L. A. M., van den Akker, E., von Lindern, M., & Wahl, S. A. (2022). Expansion and differentiation of ex vivo cultured erythroblasts in scalable stirred bioreactors. *Biotechnology and Bioengineering*, 119, 3096–3116. <https://doi.org/10.1002/bit.28193>